binding to CA (Bukovsky et al., 1997). In order to further elucidate the role of CypA and CA interactions in the antiviral activity of CypA, we investigated whether HIV-1 mutant (NL-ScaVR) or HIV-2 (GH123), whose CAs are unable to bind CypA, are restricted to human and OWM cells. NL-SVR, which can bind CypA and is an HIV-1 NL43 variant carrying SIVmac vif, was used as a control virus. NL-ScaVR is a NL43 variant carrying both SIVmac vif and the SIVmac gag h4/5 loop and has been shown to be able to grow in CM cells (Kamada et al., 2006). Consistent with our previous finding, expression of TRIM5α lacking the SPRY domain enhanced HIV-1(NL-SVR, NL-ScaVR) and HIV-2 infectivity in OWM cells (Figs. 4Ad, Bd, and Cd) compared with non-interfering control (Figs. 4Ac, Bc, and Cc). Exogenous expression of CypA suppressed the NL-SVR virus, which is able to bind CypA, in OWM cells (Fig. 4Ad) but not in human cells (Fig. 4Ab). In contrast, both NL-ScaVR (Fig. 4B) and GH123 (Fig. 4C), those cannot bind CypA, were not suppressed in either human or OWM cells by exogenously expressed CypA. Instead, those viruses tended to show slightly higher titers in cells expressing exogenous CypA.

As for the CypA protein, it is known that H54, R55, and H126 are crucial for the incorporation of CypA into HIV-1 virion (Dorfman et al., 1997). When we introduced R55A substitution into an HA-tagged version of CypA, the suppressive effect of exogeneous CypA was eliminated in CV1 and LLC-MK2 cells (Fig. 5A), although the level of expression in those cells was comparable to that of wild type CypA (Fig. 5B). Expression levels of TRIM5α lacking the SPRY domain in mutant CypA and the wild type CypA expressing cells were also comparable (Fig. 5B). These results indicate that CypA and CA interaction is essential for HIV-1 restriction by CypA in OWM cells.

CypA multimerization is not required for the HIV-1 restriction in OWM cells

In a mutagenesis study of TRIMCyp, overexpression of CypA-like protein reportedly reduced susceptibility of cells to HIV-1 (Diaz-Griffero et al., 2006). Javanbakht et al. (2007) reported that multimerization of CypA increased the anti-HIV-1 activity of CypA. Thus, it is possible that multimerization of CypA occurs only in OWM cells but not in human cells. To determine the extent of multimerization of CypA in human and OWM cells, we infected 293T and LLC-MK2 cells with SeV expressing CypA-HA and fixed the cell lysates with glutaraldehyde. CypA-HA proteins were then immunoprecipitated by using the anti-HA antibody. As shown in Fig. 6, most of the CypA-HA protein was monomeric in both 293T and LLC-MK2 cells, suggesting that the multimerization of exogenous CypA is not required for HIV-1 restriction in OWM cells.

Discussion

In the study reported here, we investigated the role of CypA in HIV-1 restriction of OWM cells. We demonstrated that exogenous

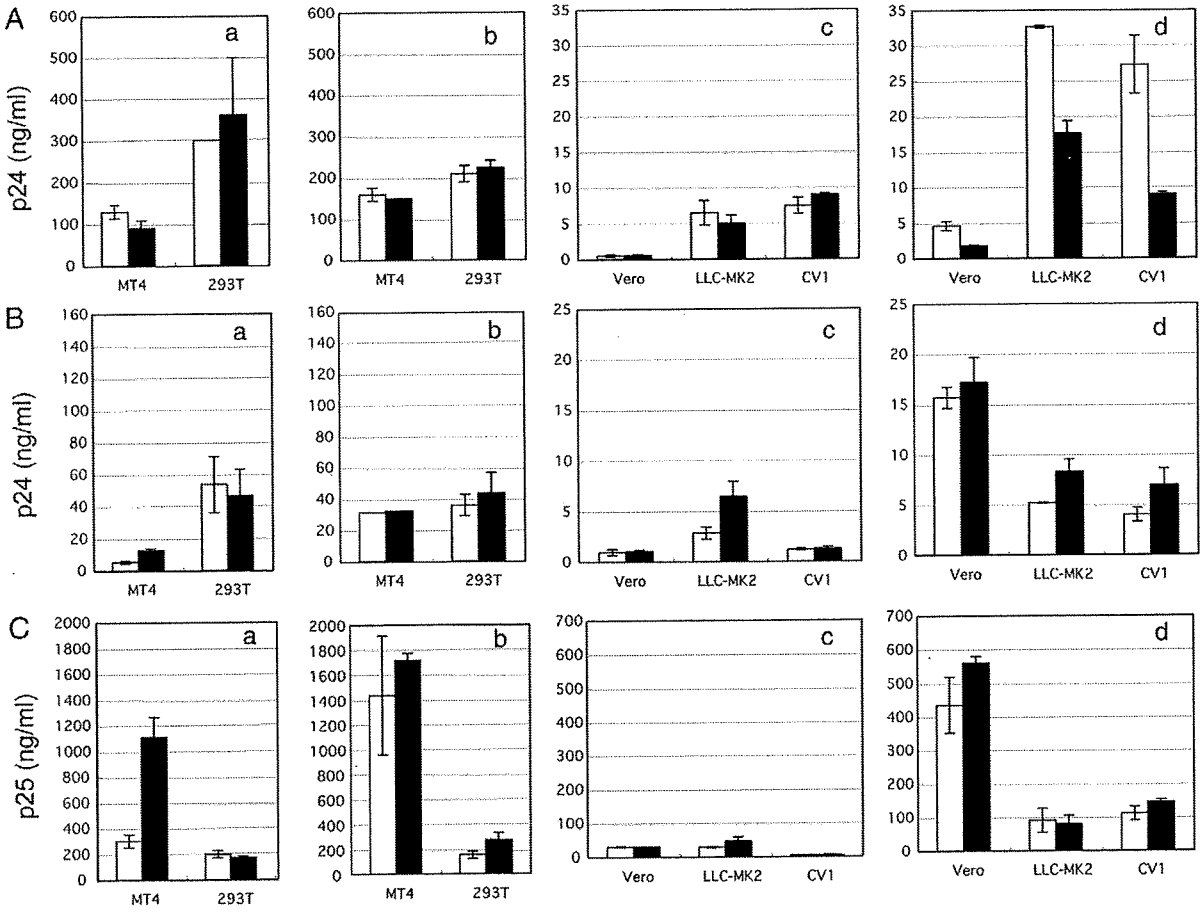

Fig. 4. MT4, 293T, Vero, LLC-MK2 and CV1 cells were infected with SeV expressing AGM TRIM5α lacking the coiled-coil domain (a and c) or CM TRIM5α lacking the SPRY domain (b and d) mixed with the empty SeV vector parental Z strain (white bars) or SeV expressing CypA (black bars), at a MOI of five PFUs per cell for each virus and incubated at 37 °C for 16 h. Cells were then superinfected with 20 ng of p24 of VSV-pseudotyped HIV-1-NL-SVR (A), HIV-1-NL-ScaVR (B) or p25 of HIV-2 GH123 (C). The culture supernatants were collected 3 days after infection, and the level of p24 or p25 was measured wth a RETROtek antigen ELISA kit. Data points show means of triplicate samples with SD.

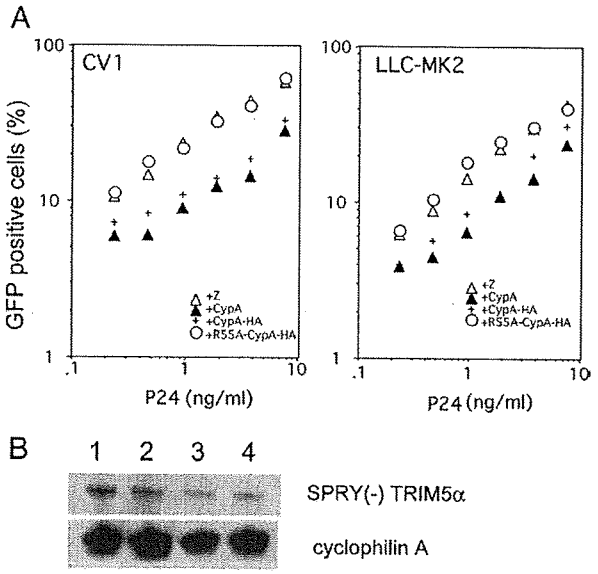

Fig. 5. (A) CV1 and LLC-MK2 cells were infected with SeV expressing CM TRIM5α lacking the SPRY(-) domain mixed with SeV expressing CypA (black triangles), CypA-HA (crosses), R55A-CypA-HA (white circles) or the empty SeV vector parental Z strain (white triangles) at a MOI of five PFUs per cell for each virus and incubated at 37 °C for 16 h. Serially diluted VSV-pseudotyped HIV-1 vectors encoding GFP were inoculated, and infected cells were counted with a flowcytometer. Representative data of at least three independent experiments is shown. (B) Lysates of CV1 (lanes 1 and 2) and LLC-MK2 (lanes 3 and 4) cells infected with SeV expressing CM TRIM5α lacking the SPRY(-) domain mixed with SeV expressing CypA-HA (lanes 1 and 3) or R55A-CypA-HA (lanes 2 and 4) were visualized by western blotting with an antibody against HA. Representative data of two independent experiments is shown.

expression of CypA suppresses HIV-1 infection in OWM cells in the absence of functional TRIM5α and that the inhibitory activity of CypA depends upon the interaction of CypA moiety with HIV-1 capsid. In addition, disruption of CypA and capsid interaction by CsA treatment enhanced the HIV-1 susceptibility of OWM cells even in the absence of functional TRIM5α. These results suggest the presence in OWM cells of TRIM5α-independent anti-HIV-1 activity mediated by CypA.

Knock-down of TRIM5 alone or dominant negative suppression of functional TRIM5α caused enhancement of HIV-1 infection and exogenous expression of CypA partially compensating for the absence of TRIM5α in HIV-1 infection, even though the expression levels of exogenous CypA were overwhelmingly higher than those of TRIM5α. This result suggests that TRIM5α may play a pivotal role in HIV-1 restriction in the OWM cells used in our study. We speculate that the mechanisms of anti-HIV-1 activity mediated by TRIM5α-independent CypA is static, for example, by trapping the virion core in cytoplasm and interfering with the nuclear transport of reverse transcription complex. Although CypA itself is not strong enough to eliminate HIV-1 infection, endogenous TRIM5α can attack HIV-1 more effectively if CypA traps virion in cytoplasm and reinforces restriction process.

Recently, two groups reported that the simultaneous knock-down of both CypA and TRIM5 in OWM cells caused minimal additional increase of HIV-1 infection compared with knock-down of TRIM5 alone, suggesting that CypA inhibits HIV-1 replication in OWM cells in a TRIM5-dependent manner. They suggested that CypA is required for CA recognition by TRIM5α. We agree that both CypA and TRIM5α are able to suppress HIV-1 infection in OWM cells, since the most potent suppression of HIV-1 infection in our study was observed in the presence of both CypA and TRIM5α. However, our findings also indicate the presence in OWM cells of TRIM5α-independent anti-HIV-1 activity mediated by CypA. At present, the reason for the discrepancy between their results and ours is not clear. It is possible that the dominant negative protein we used interfered more effectively with TRIM5α function than did the RNAi used in the other studies. In this respect, it is noteworthy that one of the two groups did observe slightly higher HIV-1 infection after simultaneous knock-down of CypA and TRIM5 than after knock-down of TRIM5 alone (Berthoux et al., 2005).

The effect of CypA on HIV-1 infection in human cells is opposite to the effect that in cells from OWM. It has been proposed that interaction of CypA with CA protects HIV-1 against restriction by human TRIM5α or other unknown antiviral factors (Luban, 2007; Towers, 2007). Our findings did not support this hypothesis that CypA protects HIV-1 from human TRIM5α, since we found that CsA treatment of human cells suppressed the HIV-1 infection even in the absence of functional human TRIM5α. In case of a virus unable to bind CypA, overexpression of CypA led to slightly higher virus replication in both human and OWM cells, although the enhancement varied among cells. It has also been reported that CypA augmented cell proliferation and gene expression in cancer cells (Li et al., 2005; Yang et al., 2005). It is possible that CypA itself affects the cell signaling or innate immune pathway to support high virus replication in both human and OWM cells. In the case of HIV-1, which is able to bind CypA, however, overexpression of CypA showed suppression of HIV-1 replication only in OWM cells. This suggests that the HIV-1 restricting activity of exogenously expressed CypA surpasses the HIV-1 enhancing effect of CypA in OWM cells. The effect of CsA treatment was more prominent in the presence of TRIM5α than in the absence of TRIM5α. It is therefore likely that CsA treatment in the presence of TRIM5α disrupted both the TRIM5α-dependent and -independent effects of CypA, whereas CsA treatment in the absence of TRIM5α disrupted only the TRIM5α-independent effect.

The amino acids sequence of human CypA is identical to the sequences of OWM CypAs. The cell type specific difference in the effect of exogenous CypA expression must thus be caused by the difference in cellular factor(s) interacting with CypA. Diaz-Griffero et al. (2007) showed exogenous expression of CypA suppressed HIV-1 in feline CRFK cells. On the other hand, Javanbakht et al. (2007) reported that multimerized CypA but not monomeric CypA suppressed HIV-1 in canine Cf2Th cells. These findings also suggest that the effect of exogenously expressed monomeric CypA on HIV-1 infection varies widely among cells or species. It is further possible that a certain OWM-specific restriction factor binds to CypA in OWM cells and thus

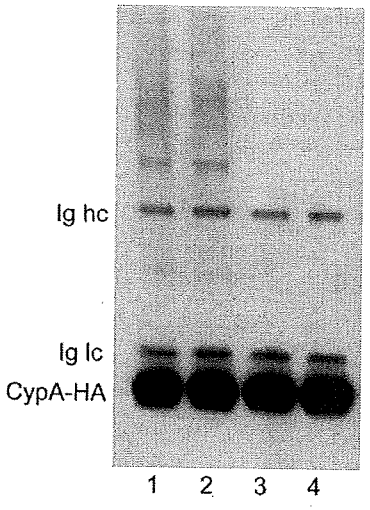

Fig. 6. Lysates of CV1 (lanes 1 and 3) and 293T (lanes 2 and 4) cells infected with SeV expressing CypA-HA were first fixed with 2.5 mM glutaraldehyde and then subjected to immunoprecipitation with an anti-HA High Affinity rat monoclonal antibody. CypA-HA proteins were visualized by western blotting with an antibody against HA. Ig hc and Ig lc indicate the IgG heavy chain and light chain used for immunoprecipitation, respectively.

inhibits HIV-1 infection. The identification of factor(s) reacting with CypA in OWM cells is therefore important to gain an understanding of the precise mechanisms of OWM resistance against HIV-1 as well as the physiological function of CypA.

Materials and methods

Cloning and expression of CypA

CypA cDNA was amplified by RT-PCR from the human T cell line MT4 by using 5′-GCGGCCGCAGCCATGGTCAACCCC-3′ as the forward primer and 5′-ACGGCGGTCTTTTCATTCGAGTTGTCC-3′ as the reverse primer. The amplified product was then cloned into pCR-2.1TOPO (Invitrogen, Carlsbad, CA) and verified for nucleotide sequence authenticity. The resultant cDNA clone served as a template for mutagenesis to generate a hemagglutinin (HA;YPYDVPDYAA) tagged version and an active site mutant which replaced the 55th arginine residue with alanine. Those cDNA fragments were then cloned into the pSeV18+b(+) vector, and recombinant SeV carrying CypA, CypA-HA tag, and R55A-CypA-HA were recovered with a slightly modified previously described method (Nakatsu et al., 2006; Nakayama et al., 2004; Takeda et al., 2005). Generation of SeV expressing CM-TRIM5α lacking the SPRY domain (CM-SPRY(-)-SeV) (Song et al., 2007) and SeV expressing AGM-TRIM5α lacking the coiled-coil domain (AGM-CC(-)-SeV) were described previously (Maegawa et al submitted).

RNA interference

Si-TRIM5 was a mixture of five siRNA targeting TRIM5: si-TRIM5-1 (5′-CUGAGAAUAUACAGCCUAAdTdT-3′), si-TRIM5-2 (5′-CGGCAGAUUUUGAGCAACUdTdT-3′), si-TRIM5-3 (5′-GCAAUGAGCUGCAGAACCUdTdT-3′), si-TRIM5-4 (5′-GGUUAUAGGGUUACAGGAAdTdT-3′) and si-TRIM5-5 (5′-GUUACAGGAAGGAGAUAAAdTdT-3′). All siRNAs were directed against AGM TRIM5 coding sequences. The 5′ ends of siTRIM5-1, -2, -3, -4, and -5 were located at positions 194, 551, 596, 1266, and 1275, respectively, of the TRIM5 open reading frame. For negative control, "SiCONTROL Non-targeting siRNA#2 (Si-Cont.)" (5′-UAAGGCUAUGAAGAGAUACUU-3′) was used (Dharmacon, Lafayette, CO). 0×10^5 CV1 cells in 6-well plates were transfected with 60 pmol of siRNA using credia-TF (Credia Japan, Kyoto, Japan) according to the manufacturer's instructions.

Real time PCR

Total RNA extracted from siRNA transfected CV1 cells were examined for the expression of TRIM5α using the TaqMan PCR method according to the manufacturer's instructions (Applied Biosystems). Sequences of the probe and primers used to specifically detect TRIM5α were as follows. forward primer: 5′-AACCTGGAGAAGGAGGAAGAAGA-3′, reverse primer: 5′-CTGGGTCTGCTGCACCAT-3′ and probe: 5′-FAM-TCCGTTTCAGACTTCG-TAMRA-3′. These primers amplify the coiled-coil region of TRIM5 gene.

Viruses and HIV-1 lentivirus vector

VSV-G-pseudo typed HIV-1-NL-SVR, HIV-1-NL-ScaVR, or HIV-2-GH123 was prepared by transfection of 293T cells with a combination of pMD.G (Miyoshi et al., 1998, 1997) and pNL-SVR (Kamada et al., 2006), pNL-ScaVR (Kamada et al., 2006) or pGH123 (Shibata et al., 1990), respectively. pNL-SVR and pNL-ScaVR were generated by PCR-based mutagenesis by using pNL432 (Adachi et al., 1986) as a template as reported by Kamada et al. (2006). HIV-1 vector expressing GFP was prepared as described previously (Miyoshi et al., 1998, 1997). Two days after transfection, culture supernatants of 293T cells were collected and assayed for their p24 or p25 level by using a RETROtek antigen ELISA kit (ZeptoMetrix Corp., Buffalo, NY).

Viral infection

Assays for the HIV-1 vector expressing GFP were performed in 24-well plates containing 4×10^4 Vero, CV1, LLC-MK2, MT4 or 293T cells. Target cells were infected with AGM-CC(-)-SeV or CM-SPRY(-)-SeV mixed with SeV expressing CypA, CypA-HA or the empty SeV vector parental Z strain at a multiplicity of infection of five plaque forming units per cell for each virus and incubated at 37 °C for 16 h. Serially diluted VSV-pseudotyped HIV-1 vectors encoding GFP were then inoculated, and infected cells were counted with a flowcytometer (FACScan, Becton Dickinson Biosciences, San Jose, CA) 40 h after infection.

4×10^4 Vero, CV1, LLC-MK2, MT4 or 293T was infected with AGM-CC(-)-SeV or CM-SPRY(-)-SeV mixed with SeV expressing CypA or the empty SeV vector parental Z strain at a multiplicity of infection of five PFUs per cell for each virus and incubated at 37 °C for 16 h. Cells were then superinfected with 20 ng of p24 of HIV-1-NL-SVR, HIV-1-NL-ScaVR or p25 of HIV-2 GH123. The culture supernatants were collected 3 days after infection, and the level of p24 or p25 was measured with the aid of a RETROtek antigen ELISA kit.

Immunoprecipitation and western blot analysis

We analyzed the expression levels of CypA in Vero, CV1, LLC-MK2, 293T or MT4 cells infected with recombinant SeV expressing CypA-HA by western blot analysis by using anti-CypA polyclonal antibody (Affinity BioReagents, Golden, CO). For analysis of the oligomeric CypA, cell lysates were first fixed with 2.5 mM glutaraldehyde and then precipitated with anti-HA High Affinity rat monoclonal antibody (Roche Diagnostics, Indianapolis, IN) as described previously (Mische et al., 2005). Materials were subjected to SDS-PAGE on a 4-12% NuPAGE Bis-Tris gel (Invitrogen) and proteins in the gel were then electronically transferred to a PVDF membrane (Immobilon; Millipore, Billerica, MA). Blots were blocked and probed with anti-HA antibody overnight at 4 °C, and then incubated with peroxidase-conjugated anti-rat IgG (American Qualex, San Clemente, CA) and developed using the Chemilumi-one L HRP chemiluminescent kit (Nacali, Kyoto, Japan). Visualized images were recorded by with LAS1000 (Fujifilm, Tokyo, Japan).

Acknowledgments

We thank Dr. Y. Yanagi and Dr. M. Takeda for their help to improve Sendai vector recovery system. We also thank S. Bandou for the technical assistance and N. Teramoto for help. This work was supported by grants from the Human Health Foundation, the Ministry of Education, Culture, Sports, Science, and Technology, and the Ministry of Health, Labour and Welfare, Japan.

References

Adachi, A., Gendelman, H.E., Koeing, S., Folks, T., Willey, R., Rabson, A., Martin, M.A., 1986. Production of acquired immunodeficiency syndrome-associated retrovirus in human and nonhuman cells transfected with an infectious molecular clone. J. Virol. 59, 284–291.

Berthoux, L., Sebastian, S., Sokolskaja, E., Luban, J., 2004. Lv1 inhibition of human immunodeficiency virus type 1 is counteracted by factors that stimulate synthesis or nuclear translocation of viral cDNA. J. Virol. 78, 11739–11750.

Berthoux, L., Sebastian, S., Sokolskaja, E., Luban, J., 2005. Cyclophilin A is required for TRIM5{alpha}-mediated resistance to HIV-1 in Old World monkey cells. Proc. Natl. Acad. Sci. U. S. A. 102, 14849–14853.

Braaten, D., Aberham, C., Franke, E.K., Yin, L., Phares, W., Luban, J., 1996a. Cyclosporine A-resistant human immunodeficiency virus type 1 mutants demonstrate that Gag encodes the functional target of cyclophilin A. J. Virol. 70, 5170–5176.

Braaten, D., Franke, E.K., Luban, J., 1996b. Cyclophilin A is required for an early step in the life cycle of human immunodeficiency virus type 1 before the initiation of reverse transcription. J. Virol. 70, 3551–3560.

Braaten, D., Luban, J., 2001. Cyclophilin A regulates HIV-1 infectivity, as demonstrated by gene targeting in human T cells. EMBO J. 20, 1300–1309.

Bukovsky, A.A., Weimann, A., Accola, M.A., Gottlinger, H.G., 1997. Transfer of the HIV-1 cyclophilin-binding site to simian immunodeficiency virus from *Macaca mulatta*

can confer both cyclosporin sensitivity and cyclosporin dependence. Proc. Natl. Acad. Sci. U. S. A. 94, 10943–10948.
Diaz-Griffero, F., Vandegraaff, N., Li, Y., McGee-Estrada, K., Stremlau, M., Welikala, S., Si, Z., Engelman, A., Sodroski, J., 2006. Requirements for capsid-binding and an effector function in TRIMCyp-mediated restriction of HIV-1. Virology 351, 404–419.
Diaz-Griffero, F., Kar, A., Lee, M., Stremlau, M., Poeschla, E., Sodroski, J., 2007. Comparative requirements for the restriction of retrovirus infection by TRIM5alpha and TRIMCyp. Virology 369, 400–410.
Dorfman, T., Weimann, A., Borsetti, A., Walsh, C.T., Gottlinger, H.G., 1997. Active-site residues of cyclophilin A are crucial for its incorporation into human immunodeficiency virus type 1 virions. J. Virol. 71, 7110–7113.
Franke, E.K., Luban, J., 1996. Inhibition of HIV-1 replication by cyclosporine A or related compounds correlates with the ability to disrupt the Gag-cyclophilin A interaction. Virology 222, 279–282.
Franke, E.K., Yuan, H.E., Luban, J., 1994. Specific incorporation of cyclophilin A into HIV-1 virions. Nature 372, 359–362.
Gamble, T.R., Vajdos, F.F., Yoo, S., Worthylake, D.K., Houseweart, M., Sundquist, W.I., Hill, C.P., 1996. Crystal structure of human cyclophilin A bound to the amino-terminal domain of HIV-1 capsid. Cell 87, 1285–1294.
Hatziioannou, T., Perez-Caballero, D., Yang, A., Cowan, S., Bieniasz, P.D., 2004. Retrovirus resistance factors Ref1 and Lv1 are species-specific variants of TRIM5alpha. Proc. Natl. Acad. Sci. U. S. A. 101, 10774–10779.
Javanbakht, H., Diaz-Griffero, F., Yuan, W., Yeung, D.F., Li, X., Song, B., Sodroski, J., 2007. The ability of multimerized cyclophilin A to restrict retrovirus infection. Virology 306, 19–29.
Kamada, K., Igarashi, T., Martin, M.A., Khamsri, B., Hatcho, K., Yamashita, T., Fujita, M., Uchiyama, T., Adachi, A., 2006. Generation of HIV-1 derivatives that productively infect macaque monkey lymphoid cells. Proc. Natl. Acad. Sci. U. S. A. 103, 16959–16964.
Keckesova, Z., Ylinen, L.M., Towers, G.J., 2004. The human and African green monkey TRIM5alpha genes encode Ref1 and Lv1 retroviral restriction factor activities. Proc. Natl. Acad. Sci. U. S. A. 101, 10780–10785.
Keckesova, Z., Ylinen, L.M., Towers, G.J., 2006. Cyclophilin A renders human immunodeficiency virus type 1 sensitive to old world monkey but not human TRIM5{alpha} antiviral activity. J. Virol. 80, 4683–4690.
Kootstra, N.A., Munk, C., Tonnu, N., Landau, N.R., Verma, I.M., 2003. Abrogation of postentry restriction of HIV-1-based lentiviral vector transduction in simian cells. Proc. Natl. Acad. Sci. U. S. A. 100, 1298–1303.
Li, M., Wang, H., Li, F., Fisher, W.E., Chen, C., Yao, Q., 2005. Effect of cyclophilin A on gene expression in human pancreatic cancer cells. Am. J. Surg. 190, 739–745.
Luban, J., 2007. Cyclophilin A, TRIM5, and resistance to human immunodeficiency virus type 1 infection. J. Virol. 81, 1054–1061.
Luban, J., Bossolt, K.L., Franke, E.K., Kalpana, G.V., Goff, S.P., 1993. Human immunodeficiency virus type 1 Gag protein binds to cyclophilins A and B. Cell 73, 1067–1078.
Mische, C.C., Javanbakht, H., Song, B., Diaz-Griffero, F., Stremlau, M., Strack, B., Si, Z., Sodroski, J., 2005. Retroviral restriction factor TRIM5alpha is a trimer. J. Virol. 79, 14446–14450.
Miyoshi, H., Blomer, U., Takahashi, M., Gage, F.H., Verma, I.M., 1998. Development of a self-inactivating lentivirus vector. J. Virol. 72, 8150–8157.
Miyoshi, H., Takahashi, M., Gage, F.H., Verma, I.M., 1997. Stable and efficient gene transfer into the retina using an HIV-based lentiviral vector. Proc. Natl. Acad. Sci. U. S. A. 94, 10319–10323.
Nakatsu, Y., Takeda, M., Kidokoro, M., Kohara, M., Yanagi, Y., 2006. Rescue system for measles virus from cloned cDNA driven by vaccinia virus Lister vaccine strain. J. Virol. Methods 137, 152–155.
Nakayama, E.E., Miyoshi, H., Nagai, Y., Shioda, T., 2005. A specific region of 37 amino acid residues in the SPRY (B30.2) domain of African green monkey TRIM5alpha determines species-specific restriction of simian immunodeficiency virus SIVmac infection. J. Virol. 79, 8870–8877.
Nakayama, E.E., Tanaka, Y., Nagai, Y., Iwamoto, A., Shioda, T., 2004. A CCR2-V64I polymorphism affects stability of CCR2A isoform. Aids 18, 729–738.
Nisole, S., Lynch, C., Stoye, J.P., Yap, M.W., 2004. A Trim5-cyclophilin A fusion protein found in owl monkey kidney cells can restrict HIV-1. Proc. Natl. Acad. Sci. U. S. A. 101, 13324–13328.
Perez-Caballero, D., Hatziioannou, T., Yang, A., Cowan, S., Bieniasz, P.D., 2005. Human tripartite motif 5alpha domains responsible for retrovirus restriction activity and specificity. J. Virol. 79, 8969–8978.
Perron, M.J., Stremlau, M., Song, B., Ulm, W., Mulligan, R.C., Sodroski, J., 2004. TRIM5alpha mediates the postentry block to N-tropic murine leukemia viruses in human cells. Proc. Natl. Acad. Sci. U. S. A. 101, 11827–11832.
Reymond, A., Meroni, G., Fantozzi, A., Merla, G., Cairo, S., Luzi, L., Riganelli, D., Zanaria, E., Messali, S., Cainarca, S., Guffanti, A., Minucci, S., Pelicci, P.G., Ballabio, A., 2001. The tripartite motif family identifies cell compartments. EMBO J. 20, 2140–2151.
Rosenwirth, B., Billich, A., Datema, R., Donatsch, P., Hammerschmid, F., Harrison, R., Hiestand, P., Jaksche, H., Mayer, P., Peichl, P., et al., 1994. Inhibition of human immunodeficiency virus type 1 replication by SDZ NIM 811, a nonimmunosuppressive cyclosporine analog. Antimicrob. Agents Chemother. 38, 1763–1772.
Sawyer, S.L., Wu, L.I., Emerman, M., Malik, H.S., 2005. Positive selection of primate TRIM5alpha identifies a critical species-specific retroviral restriction domain. Proc. Natl. Acad. Sci. U. S. A. 102, 2832–2837.
Sayah, D.M., Sokolskaja, E., Berthoux, L., Luban, J., 2004. Cyclophilin A retrotransposition into TRIM5 explains owl monkey resistance to HIV-1. Nature 430, 569–573.
Shibata, R., Miura, T., Hayami, M., Ogawa, K., Sakai, H., Kiyomasu, T., Ishimoto, A., Adachi, A., 1990. Mutational analysis of the human immunodeficiency virus type 2 (HIV-2) genome in relation to HIV-1 and simian immunodeficiency virus SIV (AGM). J. Virol. 64, 742–747.
Sokolskaja, E., Sayah, D.M., Luban, J., 2004. Target cell cyclophilin A modulates human immunodeficiency virus type 1 infectivity. J. Virol. 78, 12800–12808.
Sokolskaja, E., Berthoux, L., Luban, J., 2006. Cyclophilin A and TRIM5alpha independently regulate human immunodeficiency virus type 1 infectivity in human cells. J. Virol. 80, 2855–2862.
Song, H., Nakayama, E.E., Yokoyama, M., Sato, H., Levy, J.A., Shioda, T., 2007. A single amino acid of the human immunodeficiency virus type 2 capsid affects its replication in the presence of cynomolgus monkey and human TRIM5alphas. J. Virol. 81, 7280–7285.
Stremlau, M., Owens, C.M., Perron, M.J., Kiessling, M., Autissier, P., Sodroski, J., 2004. The cytoplasmic body component TRIM5alpha restricts HIV-1 infection in Old World monkeys. Nature 427, 848–853.
Stremlau, M., Perron, M., Welikala, S., Sodroski, J., 2005. Species-specific variation in the B30.2(SPRY) domain of TRIM5alpha determines the potency of human immunodeficiency virus restriction. J. Virol. 79, 3139–3145.
Stremlau, M., Song, B., Javanbakht, H., Perron, M., Sodroski, J., 2006. Cyclophilin A: an auxiliary but not necessary cofactor for TRIM5alpha restriction of HIV-1. Virology 351, 112–120.
Takeda, M., Ohno, S., Seki, F., Hashimoto, K., Miyajima, N., Takeuchi, K., Yanagi, Y., 2005. Efficient rescue of measles virus from cloned cDNA using SLAM-expressing Chinese hamster ovary cells. Virus Res. 108, 161–165.
Thali, M., Bukovsky, A., Kondo, E., Rosenwirth, B., Walsh, C.T., Sodroski, J., Gottlinger, H.G., 1994. Functional association of cyclophilin A with HIV-1 virions. Nature 372, 363–365.
Towers, G.J., 2007. The control of viral infection by tripartite motif proteins and cyclophilin A. Retrovirology 4, 40.
Towers, G.J., Hatziioannou, T., Cowan, S., Goff, S.P., Luban, J., Bieniasz, P.D., 2003. Cyclophilin A modulates the sensitivity of HIV-1 to host restriction factors. Nat. Med. 9, 1138–1143.
Yang, H., Li, M., Chai, H., Yan, S., Lin, P., Lumsden, A.B., Yao, Q., Chen, C., 2005. Effects of cyclophilin A on cell proliferation and gene expressions in human vascular smooth muscle cells and endothelial cells. J. Surg. Res. 123, 312–319.
Yap, M.W., Nisole, S., Lynch, C., Stoye, J.P., 2004. Trim5alpha protein restricts both HIV-1 and murine leukemia virus. Proc. Natl. Acad. Sci. U. S. A. 101, 10786–10791.
Yap, M.W., Nisole, S., Stoye, J.P., 2005. A single amino acid change in the SPRY domain of human Trim5alpha leads to HIV-1 restriction. Curr. Biol. 15, 73–78.

Journal of Virological Methods 151 (2008) 249–256

Contents lists available at ScienceDirect

Journal of Virological Methods

journal homepage: www.elsevier.com/locate/jviromet

Silencing of tripartite motif protein (TRIM) 5α mediated anti-HIV-1 activity by truncated mutant of TRIM5α

Hikoichiro Maegawa, Emi E. Nakayama, Ayumu Kuroishi, Tatsuo Shioda*

Department of Viral Infections, Research Institute for Microbial Diseases, Osaka University, 3-1 Yamadaoka, Suita-shi, Osaka 565-0871, Japan

ARTICLE INFO

Article history:
Received 25 December 2007
Received in revised form 9 April 2008
Accepted 9 April 2008
Available online 3 June 2008

Keywords:
TRIM5α
Sendai virus vector
SiRNA
Human immunodeficiency virus type 1
Knockdown
Dominant-negative

ABSTRACT

Tripartite motif protein (TRIM) 5α is a restriction factor of human immunodeficiency virus type 1 in Old World monkey cell. It was found that both naturally occurring and artificial TRIM5α variants lacking the SPRY domain could silence TRIM5α activity. Specifically, the artificial TRIM5α mutant could suppress TRIM5α activity of various primate species with even higher efficiency than could small interfering RNAs. The findings indicate that TRIM5α variants lacking the SPRY domain are useful for silencing TRIM5α activity.

1. Introduction

Human immunodeficiency virus type 1 (HIV-1) encounters post-entry block in Old World monkey (OWM) cells (Himathongkham and Luciw, 1996; Hofmann et al., 1999; Shibata et al., 1995), which is mediated by tripartite motif protein (TRIM) 5α (Stremlau et al., 2004). TRIM5 consists of RING, B-box 2, and coiled-coil domains, but only the α isoform possesses the SPRY (B30.2) domain at its C-terminus (Reymond et al., 2001). Several recombinant studies between human and rhesus monkey (Rh) TRIM5α revealed that the determinant of the species specificity lies in the SPRY domain of TRIM5α (Perez-Caballero et al., 2005; Sawyer et al., 2005; Stremlau et al., 2005; Yap et al., 2005). It was also demonstrated that a specific region in the SPRY domain of AGM TRIM5α determined species-specific restriction of SIVmac (Nakayama et al., 2005). Previous biochemical studies showed that TRIM5α binds viral capsid in a SPRY domain dependent manner (Sebastian and Luban, 2005; Stremlau et al., 2006). Since the SPRY domain is thought to recognize viral capsid, TRIM5α is the only isoform with anti-retroviral activity. Several isoforms of TRIM5 lack the SPRY domain, and a γ isoform of TRIM5 has been shown to exert a dominant-negative effect on anti-HIV-1 activity of rhesus monkey TRIM5α (Stremlau et al., 2004).

RNA interference is a potent and highly specific gene-silencing tool that is triggered by double-stranded RNAs of 21–23-nt. These small interfering (si)RNAs trigger gene silencing by binding to their target-mRNA sequences and cleaving the target, so that the use of siRNA for silencing specific genes in mammalian cells has become a standard laboratory procedure. However, the knockdown effect of siRNA greatly depends on the RNA sequence and transfection efficiency. In addition, the extent of the knockdown effect by siRNA may seriously affect conclusions drawn from study results. In this study, we applied the dominant-negative effect of TRIM5α variants lacking the SPRY domain on TRIM5α to silencing of TRIM5α mediated anti-HIV-1 activity.

2. Materials and methods

2.1. Cloning and expression of TRIM5s

African green monkey (AGM) TRIM5γ cDNA was amplified by reverse transcription-PCR from AGM CV1 cells by using 5′-GCGGC-CGCTACTATGGCTTCTGG-3′ and 5′-AGACTTGAGAGAAAACTGG-3′. The amplified products were cloned into pCR-2.1 TOPO (Invitrogen, Carlsbad, CA). A PCR-based mutagenesis was used to generate AGM TRIM5γ cDNA with a hemagulutinin (HA) tag (YPYDVPDYAA) at its N-terminus, a C-terminally HA-tagged AGM-TRIM5α lacking the coiled-coil domain (132nd to 233rd position) (AGM-TRIM5α-CC(−)-HA), and human TRIM5α with R332P

* Corresponding author. Tel.: +81 6 6879 8346; fax: +81 6 6879 8347.
E-mail address: shioda@biken.osaka-u.ac.jp (T. Shioda).

0166-0934/$ – see front matter © 2008 Elsevier B.V. All rights reserved.
doi:10.1016/j.jviromet.2008.04.012

mutation. AGM-TRIM5α carrying the myc tag at its C-terminus was described previously (Nakayama et al., 2006). The entire coding sequences of those TRIM5-tags were then transferred to the NotI site of pSeV18 + b(+). Recombinant Sendai viruses (SeVs) expressing various TRIM5-tags were obtained using a method described previously (Shioda et al., 2001). Recombinant SeVs expressing AGM-TRIM5α-HA, cynomolgus monkey (CM)-TRIM5α-HA, CM-TRIM5α-SPRY(−)-HA, and Rh-TRIM5α-HA were previously described (Kono et al., 2008; Nakayama et al., 2005; Song et al., 2007).

2.2. Immunoprecipitation and Western blot analysis

For protein expression analysis, human T-cell line MT-4 was infected with SeV at a multiplicity of infection (MOI) of 10 plaque forming unit (PFU) per cell, and incubated at 37 °C for 16 h. Cells were then lysed and lysates were subjected to sodium dodecyl sulfate-polyacrylamide gel electrophoresis (SDS-PAGE). Proteins in the gel were then transferred electronically to a membrane (Immobilon; Millipore, Billerica, MA). Blots were blocked and probed with the anti-HA High Affinity rat monoclonal antibody (Roche, Indianapolis, IN) overnight at 4 °C. Blots were then incubated with peroxidase-conjugated anti-rat IgG (American Qualex, San Clemente, CA). Bound antibodies were visualized with the chemilumi-one L chemiluminescent kit (Nacalai Tesque, Kyoto, Japan).

For co-immunoprecipitation analysis, CV1 cells were infected with recombinant SeV expressing various TRIM5s at a MOI of 5 PFU per cell, followed by incubation at 37 °C for 22 h. Cells were then lysed and TRIM5 proteins in the lysates were precipitated with the anti-myc mouse monoclonal antibody (9B11; Cell Signaling Technology, Danvers, AM) using a Protein G-immunoprecipitation kit (Roche, Indianapolis, IN). Precipitated proteins were detected with the same procedure as above except that the anti-myc mouse monoclonal antibody and peroxidase-conjugated anti-mouse IgG (Kirkegaard and Perry Laboratories, Gaithersburg, MD) were used for visualizing myc-tagged TRIM5α protein.

The anti-TRIM5 antibody was prepared by immunization of rabbit with a peptide (CRISYQPENIQPNRH) corresponding to the amino acid sequence from the 59th to 72nd position between the RING and the B-box 2 domains of AGM TRIM5α. The antigen was immunized with Freund's complete adjuvant. Sera from immunized rabbits were used as the anti-TRIM5 antibody in this study.

2.3. Virus and HIV-1 lentiviral vector

HIV-1-NL43 was prepared by transfection of 293T cells with pNL432 (Adachi et al., 1986). The HIV-1 vector expressing green fluorescence protein (GFP) (HIV-1-GFP) was prepared as described previously (Miyoshi et al., 1997, 1998). The viral titer was determined by measuring p24 with a RETROtek antigen ELISA kit (ZeptoMetrix, Buffalo, NY).

2.4. Viral infection

Serially diluted HIV-1-GFPs were inoculated into 5×10^4 CV1 cells in 24-well plates, and 40 h after infection, the infected cells were counted with a flow cytometer (FACScaliber; Becton Dickinson, Franklin Lakes, NJ).

For the HIV-1 infection assay, 2.0×10^5 MT-4 cells were infected with SeV expressing various TRIM5s. Nine hours after SeV infection, the cells were superinfected with 20 ng of p24 of HIV-1 NL43. The culture supernatants were collected 3 days after infection, and the p24 levels were measured.

2.5. RNA interference

si-TRIM5 was a mixture of five siRNA targeting TRIM5: si-TRIM5-1 (5′-CUGAGAAUAUACAGCCUAAdTdT-3′), si-TRIM5-2 (5′-CGGCAGAUUUUGAGCAACUdTdT-3′), si-TRIM5-3 (5′-GCAAUGAG-CUGCAGAACCUdTdT-3′), si-TRIM5-4 (5′-GGUUAUAGGGUUACAGG-AAdTdT-3′), and si-TRIM5-5 (5′-GUUACAGGAAGGAGAUAAAdTdT-3′). All siRNAs were directed against AGM TRIM5 coding sequences. The 5′ ends of si-TRIM5-1, si-TRIM5-2, si-TRIM5-3, si-TRIM5-4, si-TRIM5-5 were located at positions 194, 551, 596, 1266, 1275, respectively, of the TRIM5 open reading frame. For negative control, "SiCONTROL Non-targeting siRNA#2 (Si-Cont)" (5′-UAAGGCUAUGAAGAGAUACUU-3′) was used (Dharmacon, Lafayette, CO).

1.0×10^5 CV1 cells in six-well plates were transfected with 60 pmol of siRNA using credia-TF (Credia Japan, Kyoto, Japan) according to the manufacturer's recommendations. After 48 h, gene knockdown was confirmed with a previously described real-time PCR method that amplifies the coiled-coil region of TRIM5 (Nakayama et al., 2005).

To compare knockdown effect by siRNA and AGM TRIM5γ or CM-TRIM5α-SPRY(−), we prepared (1) CV1 cells transfected with Si-Cont or si-TRIM5, (2) CV1 cells infected with SeV expressing AGM TRIM5γ, CM-TRIM5α-SPRY(−) or AGM-TRIM5α-CC(−), or (3) CV1 cells transfected with si-TRIM5 and subsequently infected with SeV expressing AGM TRIM5γ, CM-TRIM5α-SPRY(−).

For the preparation of (1) cells, 1.0×10^5 CV1 cells were seeded in six-well plates. After 24 h, the cells were transfected with Si-Cont or si-TRIM5. Forty-nine hours after transfection, the cells were trypsinized, reseeded in 24-well plates, and incubated for 8 h.

For the preparation of (2) cells, 1.0×10^5 CV1 cells were seeded in six-well plates. After 72 h, the cells were infected with SeV expressing AGM TRIM5γ, CM-TRIM5α-SPRY(−) or AGM-TRIM5α-CC(−). One hour after infection, the cells were trypsinized, reseeded in 24-well plates, and incubated for 8 h.

For the preparation of (3) cells, 1.0×10^5 CV1 cells were seeded in six-well plates. After 24 h, the cells were transfected with si-TRIM5. Forty-eight hours after transfection, the cells were infected with SeV expressing AGM TRIM5γ or CM-TRIM5α-SPRY(−). One hour after infection, the cells were trypsinized, reseeded in 24-well plates, and incubated for 8 h.

These (1)–(3) cells were then infected with HIV-1-GFP. Forty hours after infection, the infected cells were counted with a flow cytometer.

2.6. Gene reporter fusion assay

A recombinant vaccinia virus (Vac)-based gene activation assay using β-galactoside gene as a reporter was performed as described previously (Nussbaum et al., 1994; Nakayama et al., 2004). Briefly, mouse fibroblast L cells were transfected with β-galactosidase reporter plasmid pGINT7β-gal and infected with a recombinant Vac expressing gp160 of an X4 HIV-1 strain NL43 or parental WR strain. At the same time, CV1 cells were infected with SeVs expressing various TRIM5s and human CXCR4, and with Vacs expressing T7 RNA polymerase and human CD4, and cultured at 31 °C overnight. Then, L and CV1 cells were mixed, incubated at 37 °C for 3 h, and β-galactosidase activities in the cell lysate were measured by using chlorophenol red-β-D-galactopyranoside as substrate.

(A)

```
AGM     TRIM5alpha 241 LQGSMMELLQGVDGIIKRIENMTLKKPKTFHKNQRRVFRAPDLKGMLDMFRELTDVRRYW 300
AGM     TRIM5gamma 241 LQGSMMELLQGVDGIIKRIENMTLKKPKTFHKNQRRVFRAPDLKGMLDMFRELTDVRRYW 300
Human   TRIM5gamma 239 LQGSVMELLQGVDGVIKRTENVTLKKPETFPKNQRRVFRAPDLKGMLEVFRELTDVRRYW 298
Rhesus  TRIM5gamma 241 LQGSMMDLLQGVDGIIKRIENMTLKKPKTFHKNQRRVFRAPDLKGMLDMFRELTDARRYW 300
CM TRIM5a-SPRY(-) 241 LQGSMMELLQGVDGIIKRIENMTLKKPKTFHKNQRRVFRAPDLKGMLDMFRELTD         296

AGM     TRIM5alpha 301 VDVTLAPNNISHAVIAEDKRQVSYQNPQIMYQAPGSLFGSLTNFNYCTGVRGSQSITSGK 360
AGM     TRIM5gamma 301 GKEKSHYHQPPCGLSLLLSLSFRILCSLLGLVF                         333
Human   TRIM5gamma 299 GKEKSHYHKPPCGLSLLLSLSFRILCSLLGSCFKIYDSPSKTHITYPSL          347
Rhesus  TRIM5gamma 301 GKEKSHYHQPPCGLSLLLSLSFRILYSLLGLVF                         333

AGM     TRIM5alpha 361 LTNFNYCTGVLGSQSITSGKHYWEVDVSKKSAWILGVCAGFQPDATYNIEQNENYQPKYG 420
AGM     TRIM5alpha 421 YWVIGLQEGDKYSVFQDGSSHTPFAPFIVPLSVIICPDRVGVFVDYEACTVSFFNITNHG 480
AGM     TRIM5alpha 481 FLIYKFSQCSFSKPVFPYLNPRKCTVPMTLCSPSS                         515
```

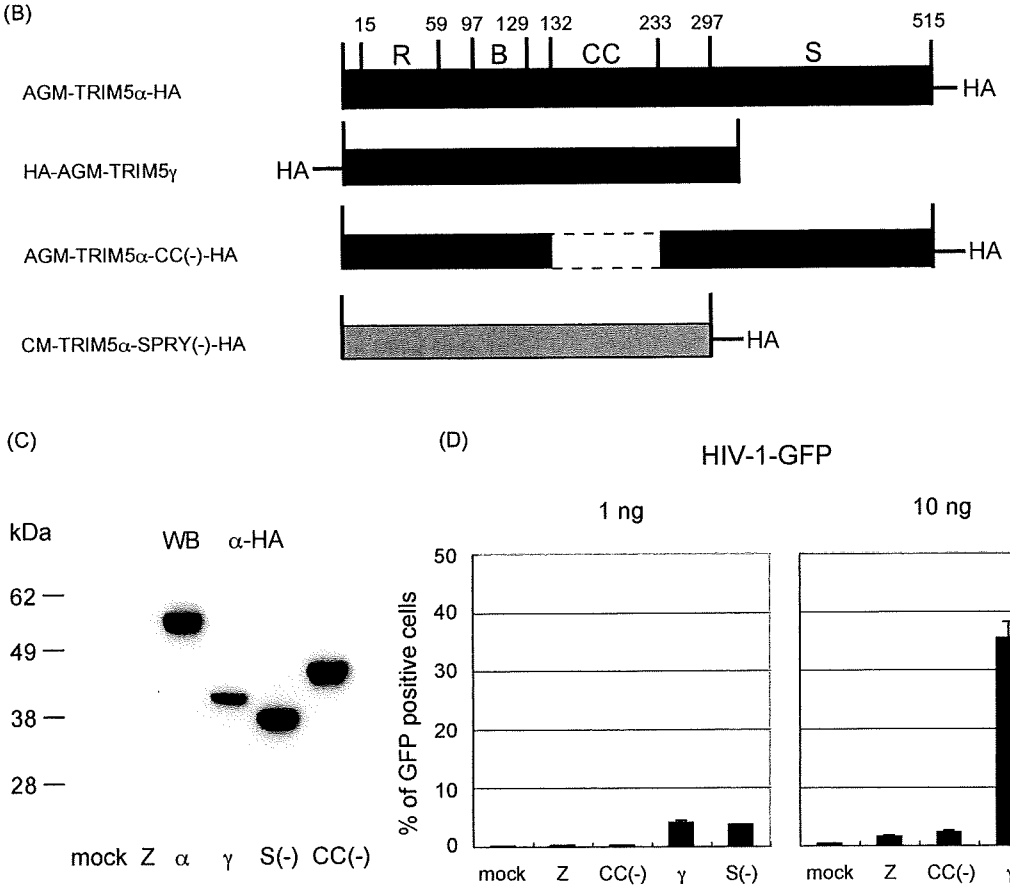

Fig. 1. (A) Alignment of amino acid sequence of the C-terminal portion of African green monkey TRIM5α (AGM TRIM5alpha), TRIM5γ (AGM TRIM5gamma), human TRIM5γ (Human TRIM5gamma), and cynomolgus monkey CM-TRIM5α lacking SPRY domain (CM-TRIM5a-S(−)) predicted from the cDNA sequences. The rhesus monkey TRIM5γ (Rhesus TRIM5gamma) sequence (Stremlau et al., 2004) is also shown. Bold face letters indicate amino acid residues in SPRY domain of AGM TRIM5α. (B) Schematic representation of TRIM5 constructs. Black and gray bars denote AGM and cynomolgus monkey (CM) sequences, respectively. *Abbreviations for domains*: R, RING; B, B-box 2; CC, coiled-coil; S, SPRY. The numbers of the amino acid residues at the boundaries of the TRIM5α domains (Song et al., 2005) are shown. Dotted boxes denote deletion of corresponding amino acid. CM-TRIM5α-SPRY(−) is composed of 296 amino acid residues. (C) Expression of various TRIM5s. TRIM5 proteins in MT-4 cells mock infected (mock) or infected with parental Z strain of SeV (Z), or with SeV expressing AGM TRIM5α (α), AGM TRIM5γ (γ), CM-TRIM5α-SPRY(−) (S(−)), and AGM-TRIM5α-coiled-coil(−) (CC(−)), at MOI of 10 PFU per cell were visualized by Western blotting with antibody to HA. (D) Dominant-negative effect of TRIM5γ and truncated mutant of TRIM5α. CV1 cells mock infected (mock) or infected with parental Z strain of SeV (Z), or with SeV expressing AGM TRIM5α (α), AGM TRIM5γ (γ), CM-TRIM5α-SPRY(−) (S(−)), or AGM-TRIM5α-CC(−) (CC(−)) at MOI of 10 PFU per cell were exposed to 1 ng (left) or 10 ng (right) of p24 of the HIV-1-GFP. GFP-positive cells were counted with a flowcytometer. Error bars show the S.D. of triplicate values for representative results of three independent experiments.

2.7. Immunofluorecence confocal microscopy

CV1 cells infected with SeV expressing several TRIM5s at MOI of 10 PFU per cell were fixed 24 h after infection in 3% paraformaldehyde in PBS, permeabilized with 0.05% saponin and 0.2% bovine serum albumin in PBS, and incubated with the anti-HA rat monoclonal antibody. Bound antibodies were then detected with the FITC-conjugated goat antibody directed against rat IgG (American Qualex Antibodies, San Clemente, CA). Indirect immunofluorescence was visualized with a Radiance 2000 laser confocal microscope system (Bio-Rad Laboratories, Hercules, CA).

For colocalization analysis, CV1 cells were infected with SeV expressing several TRIM5s at MOI of 5 PFU per cell. Colocalization of TRIM5s was visualized with the same procedure as the one described above except for the use of anti-myc mouse monoclonal antibody and Cy5-conjugated mouse antibody directed against mouse IgG (Amersham-Pharmacia Biotech, Freiburg, Germany) for visualizing myc-tagged TRIM5α protein as well as anti-HA antibody and FITC-conjugated goat antibody.

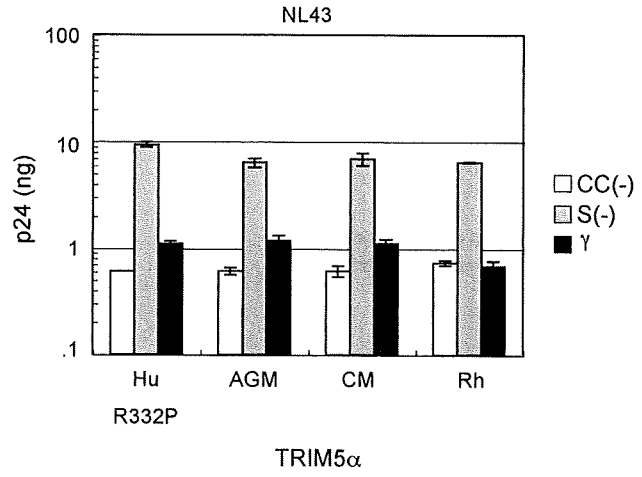

Fig. 2. Dominant-negative effect of truncated mutant of TRIM5α on TRIM5α of different primate species. MT-4 cells infected with SeV expressing indicated TRIM5α and AGM-TRIM5α-CC(−) (white bar), CM-TRIM5α-SPRY(−) (gray bar), or AGM TRIM5γ (black bar) at MOI of 5 PFU per cell were infected with NL43. Three days after infection, culture supernatants were assayed for p24 levels. The representative results of two independent experiments with similar results are shown. Error bars denote S.D. of duplicate samples.

3. Results

3.1. Dominant-negative effect of truncated mutant of TRIM5α and of TRIM5γ

Rh TRIM5γ had been shown to suppress the restriction of HIV-1 in Rh cells in a dominant-negative manner (Stremlau et al., 2004). To examine whether AGM TRIM5γ also shows a dominant-negative effect on TRIM5α-mediated HIV-1 restriction in AGM cells, TRIM5γ cDNA was cloned from AGM cell line CV1. The predicted amino acid sequence from the 241st position of TRIM5γ is shown in Fig. 1A. AGM TRIM5γ is composed of 333 amino acid residues and shares the N-terminal 300 amino acid residues with TRIM5α, while it was 16 amino acids shorter than Hu TRIM5γ. In the γ-specific region, AGM TRIM5γ showed the same amino acid sequence as that of Rh TRIM5γ except for the 326th position. A recombinant SeV expressing AGM TRIM5γ (Fig. 1B) was then constructed by first constructing AGM TRIM5γ fused with the HA tag at the C-terminus. Although AGM TRIM5γ could be detected by the anti-TRIM5 antibody in immunoblotting, it could not be detected by the anti-HA antibody (data not shown). This failure to detect the C-terminal HA tag may be due to steric hindrance of the HA tag by hydrophobic amino acid residues specific to TRIM5γ. An N-terminally HA tagged TRIM5γ was constructed and it was found that the N-terminally HA tagged TRIM5γ could be clearly detected by the anti-HA antibody at a reduced level compared to that of TRIM5α in human T-cell line MT-4 (Fig. 1C).

To examine whether AGM TRIM5γ and CM TRIM5α lacking the SPRY domain [CM-TRIM5α-SPRY(−)-HA] (Song et al., 2007), whose composition resembled that of TRIM5γ, shows a dominant-negative effect on TRIM5α-mediated HIV-1 restriction in AGM cells, CV1 cells were infected with SeV expressing HA-AGM-TRIM5γ or CM-TRIM5α-SPRY(−)-HA. Nine hours after infection, the cells were superinfected with HIV-1-GFP and infected cells were quantified by counting the GFP-positive cells. Fig. 1D shows the effect of various TRIM5 proteins on AGM TRIM5α mediated restriction. HIV-1-GFP infection was restricted in cells with both viral inoculation doses (1 ng and 10 ng of p24), while infection with the parental

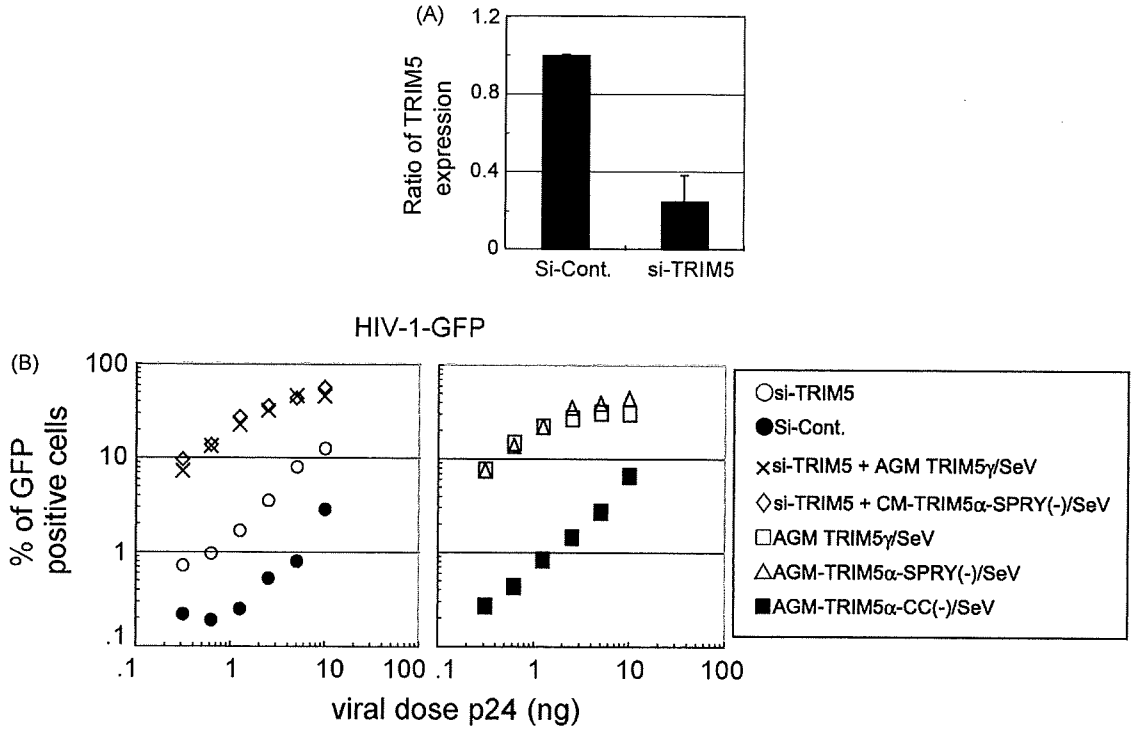

Fig. 3. (A) Reduction of TRIM5 expression by siRNA. CV1 cells were transfected with the si-TRIM5 or Si-Cont. Forty-eight hours after transfection, TRIM5 expression levels were measured by real-time PCR as described in Section 2. Data show the means of three independent experiments. Error bars denote S.D. of three independent experiments. (B) Comparison of knockdown effect by siRNA and CM-TRIM5α-SPRY(−) or AGM TRIM5γ. CV1 cells were transfected with si-TRIM5 (white circles), Si-Cont (black circles), si-TRIM5, and subsequently infected with SeV expressing AGM TRIM5γ (×) or CM TRIM5α-SPRY(−) (white diamonds) (left graph), or infected with SeV expressing AGM TRIM5γ (white squares), CM TRIM5α-SPRY(−) (white triangles), or AGM-TRIM5α-CC(−) (black squares) (right graph). These cells were then infected with HIV-1-GFP and GFP-positive cells were counted with a flowcytometer. The representative results of two independent experiments with similar results are shown.

Z strain of SeV did not affect resistance to HIV-1-GFP infection. For negative control, we used another recombinant SeV expressing AGM-TRIM5α-CC(−)-HA. Expression of this mutant TRIM5α was at a level similar to that of the wild type TRIM5α in MT-4 cells (Fig. 1C). As expected, cells infected with SeV expressing AGM-TRIM5α-CC(−) were also resistant to HIV-1-GFP infection. In contrast, cells infected with SeV expressing HA-AGM-TRIM5γ showed greatly increased sensitivity to HIV-1 infection. Cells infected with SeV expressing CM-TRIM5α-SPRY(−) also became sensitive to HIV-1 infection, while the level of the dominant-negative effect of CM-TRIM5α-SPRY(−) was similar to that of AGM TRIM5γ.

3.2. Dominant-negative effect of truncated mutant of TRIM5α or of TRIM5γ on TRIM5α of different primate species

TRIM5 variants lacking the SPRY domain were then examined whether they have a dominant-negative effect on TRIM5α of different primate species. As shown in Fig. 2, HIV-1 infection was severely restricted by CM, Rh, and AGM TRIM5αs and Hu TRIM5α with R332P (Yap et al., 2005), while HIV-1 replicated in the presence of those same primate TRIM5αs when CM-TRIM5α-SPRY(−) was expressed simultaneously. In contrast, dominant-negative effect of TRIM5γ was relatively weak in this experiment probably due to its lower expression levels (Fig. 1C). These results demonstrate that CM-TRIM5α-SPRY(−) exerts a strong dominant-negative activity on TRIM5α function from various primate species.

3.3. Comparison of silencing effect by siRNA and truncated mutant of TRIM5α or TRIM5γ

The silencing effect of CM-TRIM5α-SPRY(−) or AGM TRIM5γ was compared with that of siRNA on AGM TRIM5 (si-TRIM5). CV1 cells were transfected with si-TRIM5 and the expression levels of TRIM5α was monitored by real-time PCR (Nakayama et al., 2005). TRIM5 mRNA expression levels in the si-TRIM5 transfected CV1 cells were reduced to approximately 25% of those in CV1 cells transfected with control siRNA (Si-Cont) (Fig. 3A), indicating a quite efficient knockdown of endogenous TRIM5α by siRNA. CV1 cells transfected with Si-Cont or si-TRIM5, or those infected with SeV expressing AGM-TRIM5α-CC(−), CM-TRIM5α-SPRY(−), or AGM TRIM5γ, were superinfected with HIV-1-GFP and the infected cells were counted after 48 h. HIV-1-GFP infection in si-TRIM5 transfected cells was enhanced 3–10-fold (depending on the viral dose) compared with that in Si-Cont-transfected cells (Fig. 3B). In cells expressing CM-TRIM5α-SPRY(−), HIV-1-GFP infection was enhanced 8–30 times (depending on the viral dose) more than in cells expressing AGM-TRIM5α-CC(−) (Fig. 3B). AGM TRIM5γ showed similar effect to CM-TRIM5α-SPRY(−). Compared with cells transfected with si-TRIM5, those infected with SeV expressing CM-TRIM5α-SPRY(−) or AGM TRIM5γ were rendered more vulnerable to infection by HIV-1-GFP (2.7–3.0-fold). In addition, CV1 cells transfected with si-TRIM5 and subsequently infected with SeV expressing CM-TRIM5α-SPRY(−) or AGM TRIM5γ were more infected with HIV-1-GFP than those with si-TRIM5 alone. These results suggest that the silencing effect of TRIM5 variants lacking SPRY domain is much more efficient than that of si-TRIM5.

3.4. Exogenous expression of TRIM5α, TRIM5γ, or truncated mutant of TRIM5α did not affect an entry step of HIV-1 infection

To exclude a possibility that exogenous AGM TRIM5γ or CM TRIM5α lacking the SPRY domain could not interfere with endogenous TRIM5α but could enhance an entry step HIV-1,

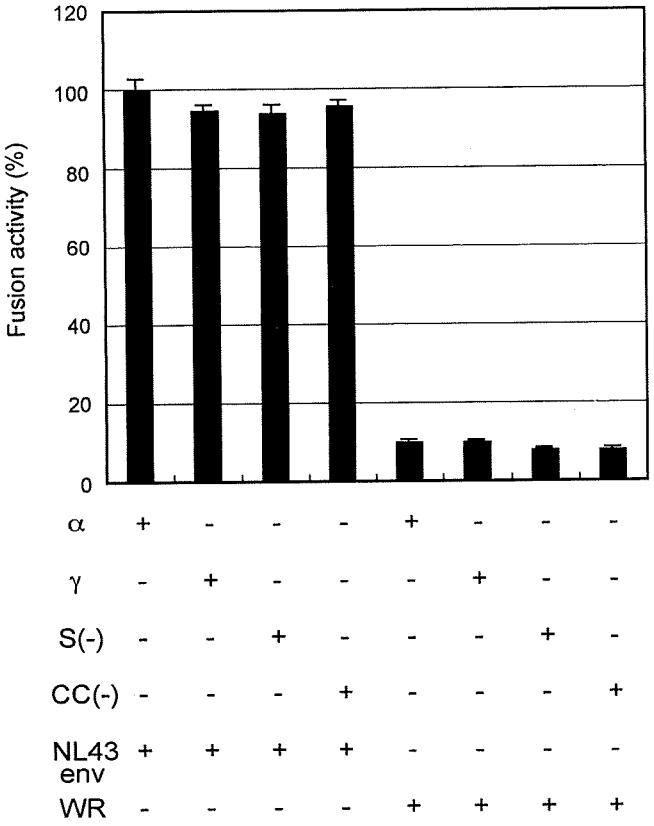

Fig. 4. Exogenous expression of TRIM5α, TRIM5γ, or truncated mutant of TRIM5α did not affect an entry step of HIV-1 infection. Mouse L cells were transfected with β-galactosidase reporter plasmid and infected with a recombinant Vac expressing NL43 envelope (env) or parental WR strain. At the same time, CV1 cells were infected with SeV expressing human CXCR4 and AGM TRIM5α (α), AGM TRIM5γ (γ), CM-TRIM5α-SPRY(−) (S(−)), or AGM-TRIM5α-coiled-coil(−) (CC(−)) and with Vacs expressing T7 RNA polymerase and human CD4. Then, L and CV1 cells were mixed, and β-galactosidase activities in the cell lysate were measured. The representative results of two independent experiments with similar results are shown. Error bars denote S.D. of triplicate samples.

a gene reported cell fusion assay was performed. CV1 cells expressing various TRIM5s, human CD4, and human CXCR4 were prepared, and those cells were mixed with mouse L cells expressing HIV-1 envelope protein. As shown in Fig. 4, cells expressing TRIM5α were equally sensitive to the envelope-mediated cell fusion to those expressing TRIM5γ or truncated mutants of TRIM5α. These results clearly indicated that TRIM5γ and truncated mutant of TRIM5α did not enhance viral entry.

3.5. Colocalization of truncated mutant of TRIM5α or TRIM5γ with TRIM5α

A confocal microscope was used to examine the subcellular localization of truncated mutant of TRIM5α or TRIM5γ. As shown in Fig. 5A, AGM TRIM5α formed cytoplasmic bodies but also exhibited diffuse cytoplasmic staining, thus confirming previous findings (Javanbakht et al., 2005). Compared with AGM TRIM5α, TRIM5γ tended to locate around the nuclear membrane to form more but smaller cytoplasmic bodies. In contrast, CM TRIM5α lacking the SPRY domain formed much larger cytoplasmic bodies than those of AGM TRIM5α, although the composition of CM TRIM5α lacking the SPRY domain resembled that of TRIM5γ. AGM TRIM5α lacking the SPRY domain [AGM-TRIM5α-SPRY(−)-HA] showed a similar subcellular localization to CM TRIM5α lacking the SPRY domain.

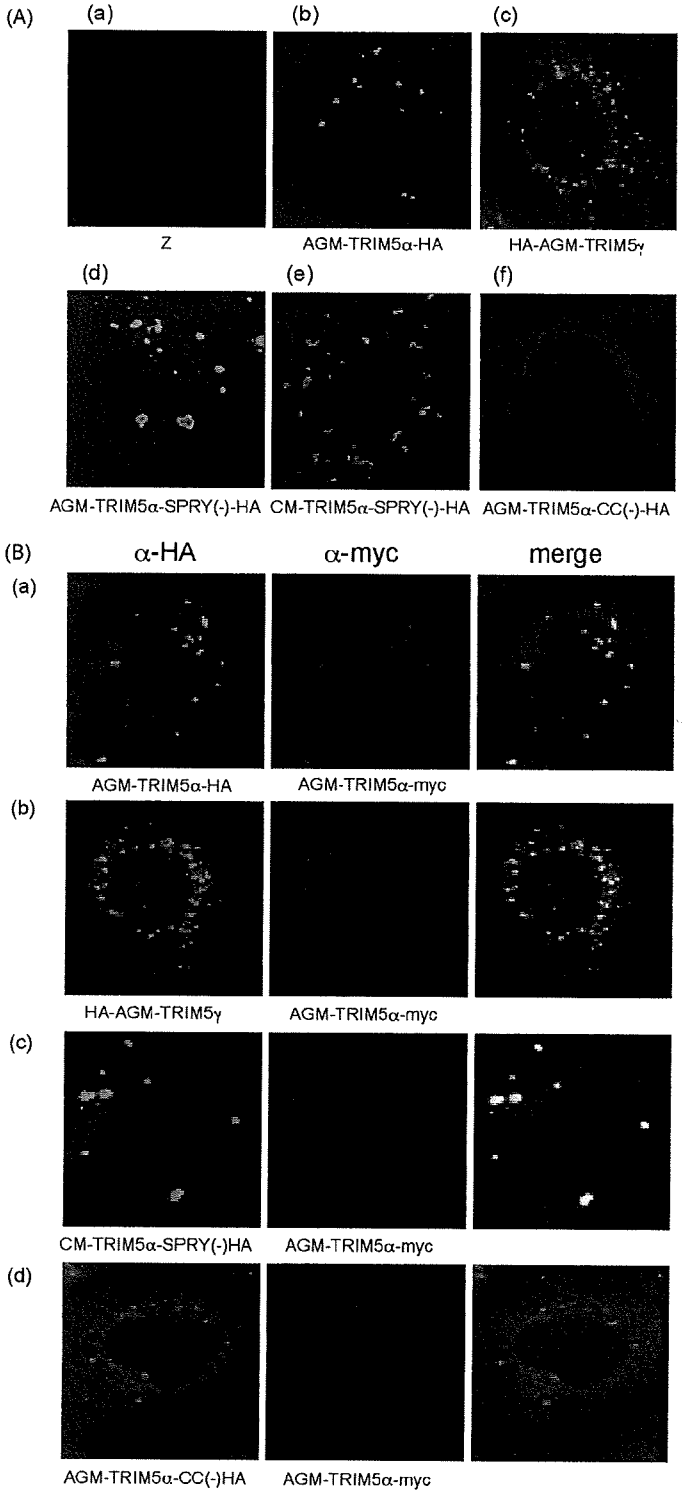

Fig. 5. (A) Subcellular localization of TRIM5s. CV1 cells infected with SeV expressing HA-tagged TRIM5 proteins at MOI of 10 PFU per cell were analyzed as described in Section 2. Representative confocal microscopic images are shown of the CV1 cells infected with parental Z strain of SeV (a), or with SeV expressing AGM TRIM5α (b), AGM TRIM5γ (c), AGM-TRIM5α-SPRY(−) (d), CM-TRIM5α-SPRY(−) (e), or AGM-TRIM5α-CC(−) (f). (B) Colocalization of HA-tagged TRIM5 variants and myc-tagged AGM TRIM5α. CV1 cells infected with SeV expressing HA-tagged TRIM5 and myc-tagged TRIM5α at MOI of 5 PFU per cell were analyzed as described in Section 2. Representative confocal microscopic images of the CV1 cells infected with SeV expressing TRIM5α-myc and SeV expressing one of the following proteins: AGM-TRIM5α-HA (a), HA-AGM-TRIM5γ (b), CM-TRIM5α-SPRY(−)-HA (c), or AGM-TRIM5α-CC(−)-HA (d). The overlay of *green* and *red* fluorescence is shown in the *right panels*.

Thus, the unique subcellular localization of TRIM5γ is due to the specific sequence of TRIM5γ and disruption of the SPRY domain causes significant changes in the subcellular localization of TRIM5α. In contrast, AGM-TRIM5α-CC(−)-HA showed diffuse cytoplasmic localization (Fig. 5A).

The subcellular localization of various TRIM5s was then examined in the presence of the wild type TRIM5α. In Fig. 5B, HA-tagged and myc-tagged proteins are shown in green (*left panels*) and red (*middle panels*), respectively. The *right panels* represent overlays of the left and middle panels. As expected, AGM-TRIM5α-HA and AGM-TRIM5α-myc colocalized in the cytoplasm (Fig. 5Ba). In cells coexpressing HA-AGM-TRIM5γ and AGM-TRIM5α-myc, both proteins exhibited minor cytoplasmic body staining around the nucleus, similar to the cytoplasmic bodies formed by HA-AGM-TRIM5γ alone (Fig. 5Bb). This result indicates that the coexpression of AGM TRIM5γ causes relocalization of AGM-TRIM5α. Colocalization of CM-TRIM5α-SPRY(−)-HA and AGM-TRIM5α-myc was observed mainly in large cytoplasmic bodies characteristic of CM-TRIM5α-SPRY(−)-HA (Fig. 5Bc). In cells coexpressing AGM-TRIM5α-CC(−)-HA and AGM-TRIM5α-myc, the former displayed diffuse cytoplasmic staining (Fig. 5Bd), while the latter formed cytoplasmic bodies. These results confirm the involvement of the coiled-coil domain in formation of the TRIM5 oligomer.

3.6. Hetero-oligomerization of truncated mutant of TRIM5α or TRIM5γ and TRIM5α

TRIM5α reportedly forms homo-trimers via the coiled-coil domain (Mische et al., 2005). To test whether truncated mutant of TRIM5α or TRIM5γ can form hetero-oligomers with TRIM5α, various HA-tagged TRIM5s and AGM-TRIM5α-myc were subjected to co-immunoprecipitation analysis. Fig. 6 shows the association of AGM-TRIM5α-HA, HA-AGM-TRIM5γ, and CM-TRIM5α-SPRY(−)-

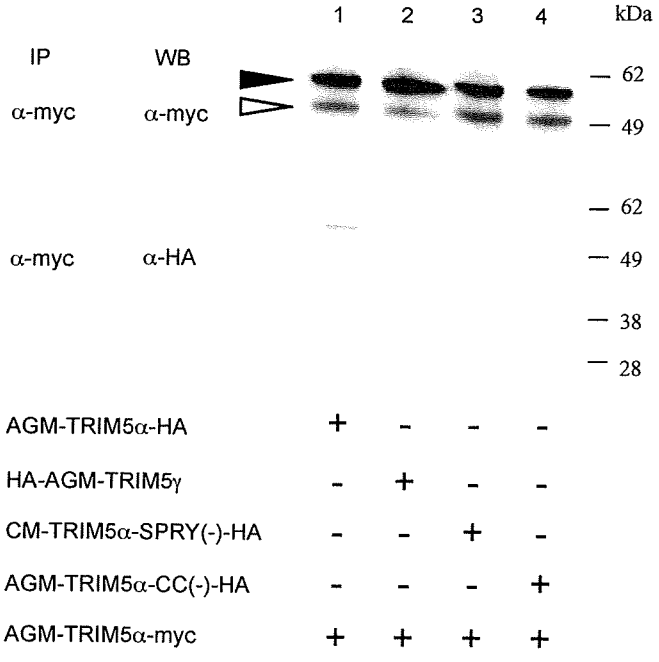

Fig. 6. Co-precipitation analysis of TRIM5 oligomerization. CV1 cells were infected with SeV expressing HA-tagged TRIM5 and myc-tagged AGM TRIM5α at MOI of 5 PFU per cell. After 22 h, the cells were lysed and subjected to immunoprecipitation with an anti-myc antibody. Immunoprecipitates were analyzed by Western blot using the antibodies indicated. Black triangles denote AGM-TRIM5α-myc proteins and white triangles non-specifically reacted proteins.

HA with AGM-TRIM5α-myc. In contrast, AGM-TRIM5α-CC(−)-HA did not show any association with AGM-TRIM5α-myc, confirming involvement of the coiled-coil domain in the self-association of TRIM5α. These results suggest that the dominant-negative effect of CM-TRIM5α-SPRY(−) or AGM TRIM5γ was due to hetero-oligomer formation that prevented binding to the target viral capsid.

4. Discussion

The application of a dominant-negative effect of truncated mutant of TRIM5α to efficient silencing of TRIM5α function without siRNA was demonstrated. Firstly, it was shown that CM TRIM5α lacking the SPRY domain had a dominant-negative effect on AGM, Rh, CM, or Hu-R332P TRIM5α mediated anti-HIV-1 activity. These results suggest that this dominant-negative effect is exerted regardless of TRIM5α primate species. Next the knockdown effect of siRNA was compared with that of TRIM5 variants lacking SPRY domain and it was found that the silencing effect of TRIM5α mediated anti-HIV-1 activity by expression of TRIM5 variants lacking SPRY domain was superior to that of si-TRIM5.

The knockdown effect of siRNA depends on target sequence and transfection efficiency. It was shown previously that HIV-1-GFP infections in Rh cells transduced with vector expressing TRIM5γ is lower than that of Rh cells transfected with the siRNA directed against Rh TRIM5α (Stremlau et al., 2004). The difference between the result of this previous study and the present study was probably due to different expression levels of TRIM5γ. Target of the most efficient siRNA against TRIM5 were coiled-coil region in the previous study (Stremlau et al., 2004), and siRNA was also used against TRIM5α including coiled-coil region in the present study. The difference between the nucleotide sequence of AGM TRIM5α and that of CM or human is 5.9% and 10.8%, respectively, while the difference between the amino acid sequence in the coiled-coil region of AGM TRIM5α and that of CM or human is 5.9% and 9.8%, respectively. This suggests that siRNA-targeting AGM TRIM5 may not be able to knockdown TRIM5α of other primates. Compared with siRNA, the advantage of silencing by TRIM5 variants lacking the SPRY domain is that target sequence and transfection efficiency do not have to be taken into account. A retroviral gene-silencing system was developed for efficient delivery of siRNA, but it takes several weeks to establish such cell lines. For the TRIM5α study, generating only 1 SeV expressing TRIM5 variant lacking the SPRY domain proved to be quick and sufficient for silencing antiviral activity of TRIM5αs from various primate species.

Compared with TRIM5α, the subcellular localization of TRIM5γ tended to locate around the nuclear membrane while forming more but smaller cytoplasmic bodies. It has been reported that TRIM5α proteins forms trimers, whereas TRIM5γ forms dimers (Mische et al., 2005). The size of the cytoplasmic body may be affected by differences in the formation of homo-oligomers. The subcellular localization of TRIM5γ was also different from that of CM or AGM-TRIM5α-SPRY(−). Hydrophobic homopolymeric amino acids such as polyleucine have been found to aggregate in the perinuclear region (Oma et al., 2004). TRIM5γ-specific 33 amino acids contain 9 Leu, 1 Ile, 2 Phe, and 1 Val. It is thus possible that the hydrophobic nature of the TRIM5γ-specific sequence affects its subcellular localization and cytoplasmic body formation.

Many restriction factors have been identified in mammalian cells (Goff, 2004), and new information on these restriction factors may lead the development of new anti-HIV-1 strategies. Identification or characterization of new restriction factors in the absence of TRIM5α-mediated resistance can be expected to clarify the roles of other antiviral proteins. In this study, we were able to demonstrate that TRIM5 variants lacking the SPRY domain expressed by SeV showed a stronger silencing effect on TRIM5α than that expressed by siRNA regardless of primate species. It is considered that this observation can be used for studying restriction factors other than TRIM5α in a variety of mammalian cells.

Acknowledgements

We thank J. Sakuragi and S. Sakuragi for helpful discussions and S. Bando and N. Teramoto for assistance. This work was supported by grants from the Ministry of Education, Culture, Sports, Science, and Technology and the Ministry oh Health, Labor and Welfare, Japan.

References

Adachi, A., Gendelman, H.E., Koeing, S., Folks, T., Willey, R., Rabson, A., Martin, M.A., 1986. Production of acquired immunodeficiency syndrome associated retrovirus in human and nonhuman cells transfected with an infectious molecular clone. J. Virol. 59, 284–291.

Goff, S.P., 2004. Retrovirus restriction factors. Mol. Cell 16, 849–859.

Himathongkham, S., Luciw, P.A., 1996. Restriction of HIV-1 (subtype B) replication at the entry step in rhesus macaque cells. Virology 219, 485–488.

Hofmann, W., Schubert, D., LaBonte, J., Munson, L., Gibson, S., Scammell, J., Ferrigno, P., Sodroski, J., 1999. Species-specific, postentry barriers to primate immunodeficiency virus infection. J. Virol. 73, 10020–10028.

Javanbakht, H., Diaz-Griffero, F., Stremlau, M., Si, Z., Sodroski, J., 2005. The contribution of RING and B-box 2 domains to retroviral restriction mediated by monkey TRIM5α. J. Biol. Chem. 280, 26933–26940.

Kono, K., Song, H., Shingai, Y., Shioda, T., Nakayama, E.E., 2008. Comparison of antiviral activity of rhesus monkey and cynomolgus monkey TRIM5αs against HIV-2 infection. Virology 373, 447–456.

Mische, C.C., Javanbakth, H., Song, B., Diaz-Griffero, F., Stremlau, M., Strack, B., Si, Z., Sodroski, J., 2005. Retroviral restriction factor TRIM5<alpha>is a trimer. J. Virol. 79, 14446–14450.

Miyoshi, H., Takahashi, M., Gage, F.H., Verma, I.M., 1997. Stable and efficient gene transfer into the retina using an HIV-based lentiviral vector. Proc. Natl. Acad. Sci. U.S.A. 94, 10319–10323.

Miyoshi, H., Blomer, U., Takahashi, M., Gage, F.H., Verma, I.M., 1998. Development of a self-inactivating lentivirus vector. J. Virol. 72, 8150–8157.

Nakayama, E.E., Tanaka, Y., Nagai, Y., Iwamoto, A., Shioda, T., 2004. A CCR2-V64I polymorphism affects stability of CCR2A isoform. AIDS 18, 729–738.

Nakayama, E.E., Miyoshi, H., Nagai, Y., Shioda, T., 2005. A specific region of 37 amino acid residues in the SPRY (B30.2) domain of African green monkey TRIM5α determines species-specific restriction of simian immunodeficiency virus SIVmac infection. J. Virol. 79, 8870–8877.

Nakayama, E.E., Maegawa, H., Shioda, T., 2006. A dominant-negative effect of cynomolgus monkey tripartite motif protein TRIM5α on anti-simian immunodeficiency virus SIVmac activity of an African green monkey orthologue. Virology 350, 158–163.

Nussbaum, O., Broder, C.C., Berger, E.A., 1994. Fusogenic mechanism of envelope-virus glycoproteins analyzed by a novel recombinant vaccinia virus-based assay quantitating cell fusion-dependent reporter gene activation. J. Virol. 68, 5411–5422.

Oma, Y., Kino, Y., Sasagawa, N., Ishiura, S., 2004. Intracellular localization of homopolymeric amino acid-containing proteins expressed in mammalian cells. J. Biol. Chem. 279, 21217–21222.

Perez-Caballero, D., Hatziioannou, T., Yang, A., Cowan, S., Bieniarz, P.D., 2005. Human tripartite motif 5α domains responsible for retrovirus restriction activity and specificity. J. Virol. 79, 8969–8978.

Reymond, A., Meroni, G., Fantozzi, A., Merla, G., Cairo, S., Luzi, L., Riganelli, D., Zanaria, E., Messali, S., Cainarca, S., Guffanti, A., Minucci, S., Pelicci, P.G., Ballabio, A., 2001. The tripartite motif family identifies cell compartments. EMBO J. 20, 2140–2151.

Sawyer, S.L., Wu, L.I., Emerman, M., Malik, H.S., 2005. Positive selection of primate TRIM5α identifies a critical species-specific retroviral restriction domain. Proc. Natl. Acad. Sci. U.S.A. 102, 2832–2837.

Sebastian, S., Luban, J., 2005. TRIM5alpha selectively binds a restriction-sensitive retroviral capsid. Retrovirology 2, 40.

Shibata, R., Sakai, H., Kawamura, M., Tokunaga, K., Adachi, A., 1995. Early replication block of human immunodeficiency virus type 1 in monkey cells. J. Gen. Virol. 76, 2723–2730.

Shioda, T., Nakayama, E.E., Tanaka, Y., Xin, X., Liu, H., Kawana-Tachikawa, A., Kato, A., Sakai, Y., Nagai, Y., Iwamoto, A., 2001. Naturally occurring deletional mutation in the C-terminal cytoplasmic tail of CCR5 affects surface trafficking of CCR5. J. Virol. 75, 3462–3468.

Song, B., Javanbakht, H., Perron, M., Park, D.H., Stremlau, M., Sodroski, J., 2005. Retrovirus restriction by TRIM5α variants from Old World and New World Primates. J. Virol. 79, 3930–3937.

Song, H., Nakayama, E.E., Yokoyama, M., Sato, H., Levy, J.A., Shioda, T., 2007. A single amino acid of the human immunodeficiency virus type 2 capsid affects its replication in the presence of cynomolgus monkey and human TRIM5αs. J. Virol. 81, 7280–7285.

Stremlau, M., Owens, C.M., Perron, M.J., Kiessling, M., Autissier, P., Sodroski, J., 2004. The cytoplasmic body component TRIM5α restricts HIV-1 infection in Old World monkeys. Nature 427, 848–853.

Stremlau, M., Perron, M., Welikala, S., Sodroski, J., 2005. Species-specific variation in the B30.2 (SPRY) domain of TRIM5α determines the potency of human immunodeficiency virus restriction. J. Virol. 79, 3139–3145.

Stremlau, M., Perron, M., Lee, M., Li, Y., Song, B., Javanbakht, H., Diaz-Griffero, F., Anderson, D.J., Sundquist, W.I., Sodroski, J., 2006. Specific recognition and accelerated uncoating of retroviral capsids by the TRIM5α restriction factor. Proc. Natl. Acad. Sci. U.S.A. 103, 5514–5519.

Yap, M.W., Nisole, S., Stoye, J.P., 2005. A single amino acid change in the SPRY domain of human Trim5alpha leads to HIV-1 restriction. Curr. Biol. 15, 73–78.

Journal of General Virology (2008), 89, 554–566 DOI 10.1099/vir.0.83186-0

Impact of glycosylation on antigenicity of simian immunodeficiency virus SIV239: induction of rapid V1/V2-specific non-neutralizing antibody and delayed neutralizing antibody following infection with an attenuated deglycosylated mutant

Chie Sugimoto,[1,2,3] Emi E. Nakayama,[4] Tatsuo Shioda,[4] Francois Villinger,[5] Aftab A. Ansari,[5] Naoki Yamamoto,[1] Yasuo Suzuki,[3,6] Yoshiyuki Nagai[7] and Kazuyasu Mori[1,2,3]

Correspondence
Kazuyasu Mori
mori@nih.go.jp

[1]AIDS Research Center, National Institute of Infectious Diseases, Shinjuku-ku, Tokyo 162-8640, Japan

[2]Tsukuba Primate Research Center, National Institute of Biomedical Innovation, Tsukuba, Ibaraki 305-0843, Japan

[3]CREST, Japan Science and Technology Agency, Kawaguchi, Saitama 332-0012, Japan

[4]Department of Viral Infections, Research Institute for Microbial Diseases, Osaka University, Suita, Osaka 565-0871, Japan

[5]Department of Pathology and Laboratory Medicine, Emory University, Atlanta, GA 30322, USA

[6]Department of Biomedical Sciences, College of Life and Health Sciences, Chubu University, Kasugai, Aichi 487-8501, Japan

[7]Center of Research Network for Infectious Diseases, Riken, Chiyoda-ku, Tokyo 100-0006, Japan

Infection of rhesus macaques with a deglycosylation mutant, Δ5G, derived from SIV239, a pathogenic clone of simian immunodeficiency virus (SIV), led to robust acute-phase viral replication followed by a chronic phase with undetectable viral load. This study examined whether humoral responses in Δ5G-infected animals played any role in the control of infection. Neutralizing antibodies (nAbs) were elicited more efficiently in Δ5G-infected animals than in SIV239-infected animals. However, functional nAb measured by 90 % neutralization was prominent in only two of the five Δ5G-infected animals, and only at 8 weeks post-infection (p.i.), when viral loads were already below 10^4 copies ml^{-1}. These results suggest a minimal role for nAbs in the control of the primary infection. In contrast, whilst Ab responses to epitopes localized to the variable loops V1/V2 were detected in all Δ5G-infected animals at 3 weeks p.i., this response was associated with a concomitant reduction in Ab responses to epitopes in gp41 compared with those in SIV239-infected animals. These results suggest that the altered surface glycosylation and/or conformation of viral spikes induce a humoral response against SIV that is distinct from the response induced by SIV239. More interestingly, whereas V1/V2-specific Abs were induced in all animals, these Abs were associated with vigorous Δ5G-specific virion capture ability in only two Δ5G-infected animals that exhibited a functional nAb response. Thus, whereas the deglycosylation mutant infection elicited early virion capture and subsequent nAbs, the responses differed among animals, suggesting the existence of host factors that may influence the functional humoral responses against human immunodeficiency virus/SIV.

Received 25 May 2007
Accepted 7 October 2007

INTRODUCTION

The precise role of antibody (Ab) responses in the containment of human immunodeficiency virus (HIV) remains a subject of intense study and debate. Besides the classical direct virus neutralization properties, antibodies are also capable of blocking infection via other pathways such as antibody-dependent complement-mediated inactivation of virus (Aasa-Chapman *et al.*, 2005) and antibody-dependent cellular lysis (Ahmad & Menezes, 1996; Forthal *et al.*, 2001). Acquiring an understanding of these various mechanisms for their exploitation in the

development of candidate vaccines has been a major challenge.

The envelope protein (Env) of HIV/simian immunodeficiency virus (SIV) comprises an exterior protein (gp120) and a transmembrane (TM) protein (gp41), and trimers of the gp120/gp41 complexes form viral spikes that promote binding to receptors and co-receptors on the cell membrane for entry into the target cells (Wyatt & Sodroski, 1998). The major viral receptors of HIV/SIV include CD4 and a variety of co-receptors such as CCR5 or CXCR4. One desirable target epitope for neutralizing antibody (nAb) that shows relative conservation across clades is the binding site for the co-receptor (Burton *et al.*, 2004; Zolla-Pazner, 2004); however, this site is conformationally cryptic within the viral spike up until immediately after binding of the viral spike to CD4, providing an effective shielding mechanism to the virus. Another distinct feature of HIV/SIV Env is the extensive glycosylation that also effectively prevents access to antibodies directed at the epitopes (Chen *et al.*, 2005; Wyatt & Sodroski, 1998; Wyatt *et al.*, 1998). The gp120 protein possesses 18–33 Asn–X–Ser/Thr sequences, signals for the attachment of *N*-linked carbohydrate side chains (Leonard *et al.*, 1990; Ohgimoto *et al.*, 1998; Regier & Desrosiers, 1990; Zhang *et al.*, 2004). As the carbohydrate moiety is generally weakly immunogenic and is recognized to a large extent as self by the host immune system, the massive glycans on the surface of viral spikes constitute an immunologically silent facade (Wyatt & Sodroski, 1998; Wyatt *et al.*, 1998). As a result, mature viral spikes are protected from nAb and other host immune responses by a massive carbohydrate 'glycan shield' (Chen *et al.*, 2005; Wyatt & Sodroski, 1998; Wyatt *et al.*, 1998). In fact, a prominent role of carbohydrates of HIV/SIV in evasion from immune surveillance has been reported previously as follows. Variants of SIV that have evolved to acquire additional glycans in the variable regions of Env have increased neutralization resistance compared with the parental virus (Chackerian *et al.*, 1997; Cheng-Mayer *et al.*, 1999). Similarly, the appearance of neutralization escape mutants has been associated with altered glycosylation in HIV-1 evolved during the course of infection (Wei *et al.*, 2003). Conversely, infection with SIV239 mutants with deglycosylated Env (lacking *N*-linked glycosylation sites) in the variable loops V1/V2 of gp120 elicited markedly increased titres of nAb (Reitter *et al.*, 1998). We have reported that a deglycosylation mutant, Δ5G, lacking *N*-linked glycosylation sites at aa 79, 146, 171, 460 and 479 in gp120 of SIV239 displayed an attenuated phenotype when used to infect rhesus macaques (Mori *et al.*, 2001; Ohgimoto *et al.*, 1998). In addition, animals infected with Δ5G exhibited almost sterile protection against rechallenge with SIV239 (Mori *et al.*, 2001).

Thus, we suggest that studies aimed at identifying the mechanisms underlying the early and potent immune control of deglycosylated SIV may provide knowledge for the formulation of effective HIV/SIV vaccines. Studies performed herein were therefore directed at attempts to define more precisely the early humoral responses (both virus-specific nAb and non-nAb) generated after infection with Δ5G in rhesus macaques and to compare these responses with those observed in macaques inoculated with wild-type SIV239, with the rationale that results from such studies may help to identify their potential contribution towards viral control of primary infection.

METHODS

Viruses. The molecular pathogenic clone of SIV239 (Regier & Desrosiers, 1990) and its derived deglycosylated mutant, Δ5G, were used in this study. Δ5G was derived by mutagenesis of an SIV239 infectious DNA clone so that the asparagine residues for *N*-glycosylation at aa 79, 146, 171, 460 and 479 in gp120 were converted to glutamine residues (Fig. 1a) (Ohgimoto *et al.*, 1998). Viral stocks of SIV239 and Δ5G were prepared as reported previously (Mori *et al.*, 2001).

Peptides. A series of 72 consecutive 25 mer peptides overlapping by 13 aa were synthesized based on the entire SIV239 Env sequence (Env-1–72). These peptides were synthesized by the Microchemical Facility, Emory University School of Medicine, Atlanta, USA. Another set of 15 mer peptides overlapping by 11 aa around the V1/V2 region in gp120 (V1V2-1–12) was synthesized by Sigma-Aldrich Japan based on the Δ5G sequence (see Fig. 5b). All peptides were dissolved in DMSO diluted in PBS.

Animal infection. Juvenile rhesus macaques originating from Myanmar (Burma) (Mm12, Mm13, Mm20, Mm23 and Mm26) or from Laos (Mm07, Mm22 and Mm25) were used following the results of screening for SIV, simian T-cell lymphotropic virus, B virus and type D retrovirus infection, which were all negative prior to inception of the study. All animals were housed in individual cages and maintained according to the rules and guidelines for experimental animal welfare as outlined by the National Institute of Infectious Diseases and National Institute of Biomedical Innovation. Animals were infected intravenously with Δ5G or SIV239 as described previously (Mori *et al.*, 2001).

Plasma viral load measurements. SIV infection was monitored by measuring the plasma viral RNA load using a highly sensitive quantitative real-time RT-PCR. Viral RNA was isolated from plasma samples from infected animals using a commercial viral RNA isolation kit (Roche Diagnostics). SIV *gag* RNA was amplified and quantified using a method originally developed by Hofmann-Lehmann *et al.* (2000) using a TaqMan EZ RT-PCR kit (Applied Biosystems). The detection sensitivity of plasma viral RNA by this method was 100 viral RNA copies per ml plasma (given as copies ml^{-1}).

Neutralization assay. SIV neutralization was tested according to a protocol using CEMx174/SIVLTR-SEAP cells, originally described by Means *et al.* (1997). To measure low levels of nAb, IgG was purified from plasma as described below and concentrated virus stocks were used.

Anti-gp120 Ab ELISA and anti-Env peptide ELISA. Recombinant SIV239 gp120 and Δ5G gp120 were expressed utilizing a Sendai virus vector as described previously (Mori *et al.*, 2005; Yu *et al.*, 1997). Culture supernatant containing approximately 2 μg secreted SIV gp120 ml^{-1} was diluted with an equal amount of PBS, dispensed into each well of an ELISA plate and allowed to incubate at 4 °C overnight.

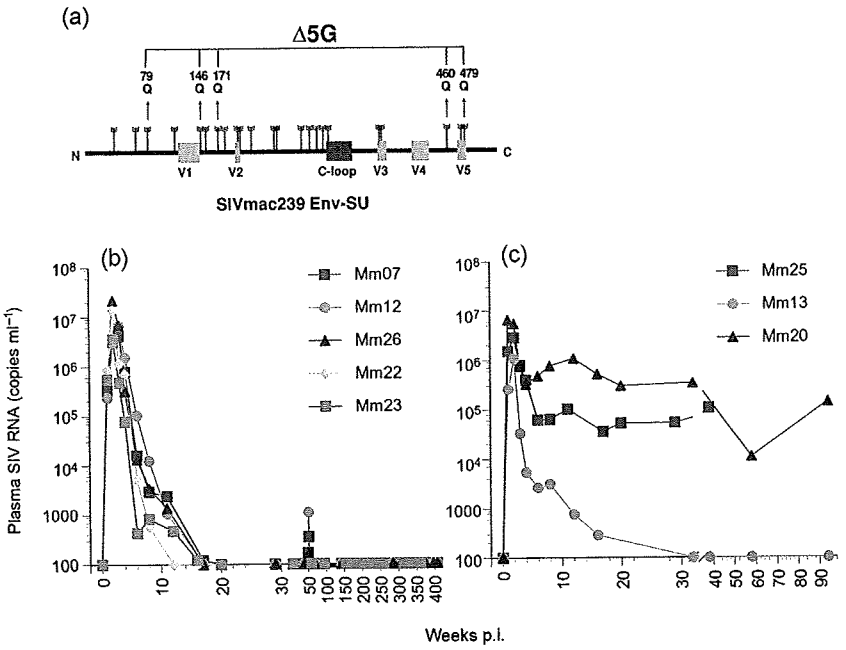

Fig. 1. Plasma SIV RNA loads in animals infected with Δ5G or SIV239. (a) *N*-Glycosylation sites in SIV239 gp120 and deglycosylation sites in Δ5G gp120. The locations of 23 *N*-glycosylation sites in SIV239 gp120, variable regions (V1–V5) and cysteine loops (C-loop) are shown. Δ5G was deglycosylated by N→Q substitutions at aa 79, 146, 171, 460 and 479 in Env (Ohgimoto *et al.*, 1998). (b, c) Plasma viral load in Δ5G-infected (b) and SIV239-infected (c) animals was measured in plasma samples using sensitive real-time RT-PCR to indicate when viral loads declined below 100 copies ml^{-1}. Three Δ5G-infected animals (Mm07, Mm12 and Mm26) were challenged with SIV239 at 48 weeks p.i.; thus, slightly increased viral loads were detected in those animals during weeks 49–51 p.i. (Mori *et al.*, 2001).

For the peptide ELISA, each peptide was diluted to 0.5 μM with 50 mM carbonate buffer (pH 9.5) and captured on Nunc Immobilizer amino plates (Nalge Nunc) at 4 °C overnight. A 1 : 100 dilution (150 μl) of the plasma sample to be tested was dispensed into antigen-immobilized plates and incubated at 37 °C for 1 h. Ab responses were detected using peroxidase-conjugated goat anti-monkey IgG and *o*-phenylenediamine. Absorbance was measured at 490 nm.

Removal of linear V1/V2 epitope-specific Abs from IgG fractions. A mixture of the peptides (V1V2-9, -10 and -11; see Fig. 5b) was conjugated to a HiTrap NHS-activated HP column (GE Healthcare). IgGs from plasma samples were fractionated using a mAb trap kit (GE Healthcare) and applied to the peptide-conjugated column. The flow-through fractions devoid of anti-V1V2-9, -10 and -11 peptide-specific Abs were collected. The concentration of IgG was determined using a protein assay kit (Bio-Rad).

Virion capture assay. The virion capture assay was modified using a method reported by Nyambi *et al.* (1998). ELISA plates were coated with the IgG samples described above at a concentration of 20 μg ml^{-1} in 50 mM carbonate buffer (pH 9.5) and incubated at 4 °C for 48 h. The plates were washed three times with PBS and blocked with 3 % BSA in PBS at 37 °C for 1 h. The plates were then washed three times with serum-free RPMI 1640. Δ5G or SIV239 virion solutions with a $p27^{gag}$ concentration of 15, 7.5 and 3.75 ng in 10 % fetal bovine serum/RPMI 1640 were added to each well of the IgG-coated plate and incubated at 37 °C for 3 h. The wells were washed five times with serum-free RPMI 1640 to remove unbound virus. The virus bound to IgG was lysed using MagNA Pure LC Lysis/Binding Buffer (Roche Diagnostics). The viral lysates were subjected to viral RNA purification using a MagNA Pure Compact nucleic acid purification kit (Roche Diagnostics). The copy number of the isolated SIV RNA was determined by real-time RT-PCR for SIV239 as described above.

Statistical analysis. Correlation analysis was done using Spearman's non-parametric rank test and the Mann–Whitney test using GraphPad Prism 4.0 software. Correlations were considered to be statistically significant for values of $P<0.05$.

RESULTS

Plasma viral loads of a quintuple deglycosylated SIV239 mutant in rhesus macaques

Eight rhesus macaques were infected intravenously with Δ5G ($n=5$) or SIV239 ($n=3$) (Mori *et al.*, 2001). Plasma viral RNA loads were assayed for up to 400 weeks p.i. and the data obtained in the Δ5G-infected (Fig. 1b) or SIV239-infected (Fig. 1c) animals were plotted. Both Δ5G and SIV239 replicated with similar kinetics during the early phase of primary infection for up to 4 weeks p.i. However, subsequent to this acute infection phase, virus replication was markedly different in the two groups of monkeys: SIV239-infected animals exhibited viral load set points around 10^5 copies ml^{-1} in two of three animals, with one animal (Mm13) having an undetectable viral load (<100 copies ml^{-1}) by 30 weeks p.i. (Fig. 1c). In contrast, the Δ5G-infected animals showed uniformly controlled viraemia reaching undetectable levels by 12–16 weeks p.i. and maintained this control for more than 6 years p.i. (Fig. 1b).

nAb response in Δ5G-infected animals

Although failure to detect a nAb response is characteristic of SIV239-infected rhesus macaques (Johnson *et al.*, 2003; Means *et al.*, 1997), the rapid control of viraemia in Δ5G-infected animals prompted us to determine whether nAb played a role in this control of viraemia. We hypothesized that the deglycosylation might lead to the elicitation of a markedly more vigorous nAb response than infection with SIV239. To maximize the detection sensitivity of weak nAb responses at early time points p.i., an assay that measures neutralization titres based on 50 % inhibition of virus replication (IC_{50}) in $CD4^+$ T-cell lines was initially used.

Consistent with the reported results in SIV239-infected animals, no appreciable nAb titre was detected in two animals (Mm13 and Mm25), despite the fact that viral load in Mm13 was distinctively decreased by 30 weeks p.i. However, we observed a rare animal (Mm20) that elicited a robust nAb response against SIV239 and a relatively delayed nAb response against Δ5G, despite the maintenance of a high viral load (Fig. 2a). These results indicated the lack of correlation of nAb response with viral load in SIV239-infected animals. In contrast, nAb was detected in two Δ5G-infected animals (Mm07 and Mm22) starting at 8 weeks p.i. and in two additional animals (Mm12 and Mm23) at 12 weeks p.i. (Fig. 2b, left panel). These titres peaked at either 12 or 18 weeks p.i., and the peak was followed by a decrease in titre that varied among animals. Mm12 and Mm23, which exhibited nAb induction at 12 weeks p.i., had essentially low titres, whilst Mm07 and Mm22, which exhibited nAb induction at an earlier time point, maintained vigorous nAb titres of >1 : 100. Of note, plasma from Mm26 did not contain detectable levels of nAb at any time p.i. In contrast, nAb against SIV239 was not induced in any of the Δ5G-infected animals (Fig. 2b, right panel). As low-level nAb may play a role in control of virus replication, purified IgG from the plasma samples was used to measure neutralizing activity. However, the results from the purified IgG corresponding to the plasma at a 1 : 3 dilution did not change the kinetics of nAb response in Δ5G-infected animals (data not shown).

In experiments where the passive administration of monoclonal HIV nAb successfully prevented the infection of macaques with simian–human immunodeficiency virus, the results unequivocally indicated that high titres of nAb were needed to achieve such protection (Nishimura *et al.*, 2002). In consideration of these results, data were recalculated based on a cut-off value of 90 % inhibition of virus replication (IC_{90}) in $CD4^+$ T-cell lines. As a result, nAb responses were detected in only two of the animals, Mm07 and Mm22, but with titres of 1 : 100 and 1 : 500, respectively (Fig. 2b, middle panel). Next, we examined the correlation between viral load and nAb titre at 8 and 12 weeks p.i. and found that the correlation was not statistically significant (Fig. 2c).

Anti-gp120 Ab response in Δ5G-infected animals

Next, we measured binding Ab responses against gp120. When the plasma samples were assayed for levels of Ab that bound to SIV239 gp120 or Δ5G gp120, essentially identical values were obtained. Fig. 3 shows the data obtained using SIV239 gp120. Remarkably, anti-gp120 responses during the early period p.i. between the two groups of monkeys were distinct. Whereas anti-gp120-specific Ab responses

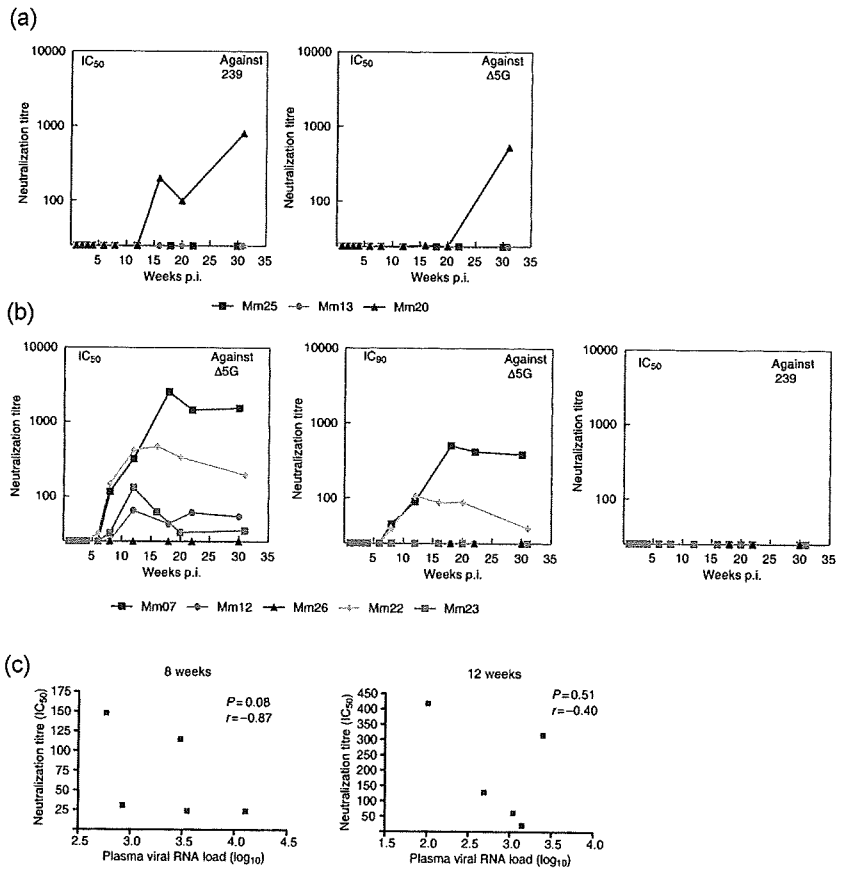

Fig. 2. nAb titres in SIV-infected animals. (a) nAb titres in SIV239-infected animals are indicated as the plasma dilution yielding 50 % inhibition (IC_{50}) of SIV239 infection (left) or Δ5G infection (right) in CEMx174/SIVLTR-SEAP cells. (b) nAb titres in Δ5G-infected animals are indicated as the plasma dilution that yielded 50 % inhibition (IC_{50}, left) and 90 % inhibition (IC_{90}, middle) of Δ5G infection or 50 % inhibition of SIV239 infection (right) in CEMx174/SIVLTR-SEAP cells. (c) Correlation between IC_{50} nAb titres and plasma viral RNA load at 8 and 12 weeks p.i. in Δ5G-infected animals.

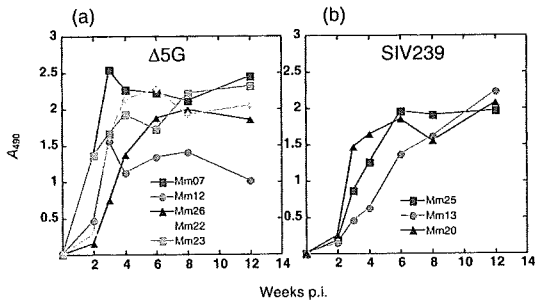

Fig. 3. Anti-gp120 Ab responses. Anti-gp120 Ab responses in Δ5G-infected (a) and SIV239-infected (b) animals were indicated as A_{490} using plasma diluted 1 : 100 in an ELISA.

peaked at 3–4 weeks p.i. in Δ5G-infected animals (Fig. 3a), those in SIV239-infected animals remained generally lower and required longer periods of time to reach their peak (Fig. 3b). Of note, whilst anti-gp120 Ab responses did not correlate well with nAb titres in the chronic phase in Δ5G-infected animals, the hierarchy detected in nAb titres (Mm07, Mm22, Mm23, Mm12 and Mm26, in descending order) was similar to that observed for gp120-binding antibodies at 2 weeks p.i. (Fig. 3a).

Ab responses to linear epitopes in gp120 and gp41 in Δ5G-infected animals differ from those detected in SIV239-infected animals

Next, we examined Ab-binding responses to linear epitopes in plasma samples from infected animals at 8 weeks p.i., as both nAb and anti-gp120-binding Ab were detected at this time point (Figs 2 and 3). We used 72 overlapping peptides encompassing the entire Env sequence of SIV239 for the detection of epitope-specific Ab in plasma samples from Δ5G-infected or SIV239-infected animals. As shown in Fig. 4 and Table 1, the plasma samples reacted with the peptides in six regions: two in gp120 and four in gp41. The regions in gp120 resided in the vicinity of V1/V2, designated region 1 (aa 109–193), and at the C terminus, designated region 2 (aa 493–529). Of note, only linear region 1 was directly affected by selected deglycosylation (aa 146 and 171). The regions in gp41 were located in the ectodomain for region 3 (aa 589–625) and region 4 (aa 660–685), and in the cytoplasmic domain for region 5 (aa 721–757) and region 6 (aa 841–879).

Although Ab responses to most of the peptides recognized in the plasma samples from Δ5G-infected animals were similar to those in SIV239-infected animals, a few peptides were recognized by Abs only in samples from Δ5G-infected animals, and Ab reactivity to some peptides was significantly different between the two groups (Fig. 4b, c and Table 1). Firstly, in region 1, whereas five peptides (Env-10, -12, -13, -14 and -15) were recognized by Abs from Δ5G-infected animals, only three peptides (Env-10, -12 and -13) reacted with Abs from SIV239-infected animals (Fig. 4b and c). Peptide Env-10 was detected by Abs from four Δ5G-infected animals, but from only one of the SIV239-infected animals. Similarly, peptides Env-12 and -13 were detected by Abs from five Δ5G-infected animals and two SIV239-infected animals. In contrast, peptides Env-14 and -15 were detected by Abs from Δ5G-infected animals but not SIV239-infected animals. The specificity of Δ5G infection in the reactivity of peptide Env-14 was statistically significant (P=0.0149) (Table 1). Secondly, the reactivity of Ab from Δ5G-infected animals with the peptides in regions 2, 3 and 4 was lower than that recorded with Ab from SIV239-infected animals (Fig. 4b and c). As shown in Table 1, the reduction in Ab reactivity from Δ5G-infected animals to peptide Env-51 (region 3) and peptide Env-56 (region 4) was significant (P=0.014 and 0.0053, respectively); however, the reduction in Ab response in region 2 was not significant. In addition, there were no significant differences in the Ab responses to the peptides in regions 5 and 6 between Δ5G-infected and SIV239-infected monkeys (Fig. 4b, c and Table 1).

A Δ5G-specific linear epitope resides in the region containing the third deglycosylation site (aa 171) between V1 and V2

As region 1 also contained the site of two mutations introduced to limit glycosylation in the Δ5G mutant, we focused additional studies on this region. To identify the Δ5G-specific epitope(s) in region 1, peptide ELISA was performed with 12 newly synthesized shorter peptides based on the Δ5G sequence spanning the V1/V2 region (Fig. 5). Ab reactivity to peptide Env-14 was mapped to peptides V1V2-9–11 (Fig. 5a). Thus, three linear epitopes (encompassed in peptides Env-10, V1V2-3 and V1V2-9–11) were identified within the V1/V2 region (Figs 4 and 5). Whilst two epitopes contained in peptides Env-10 and V1V2-3 were recognized by Ab from both SIV239- and Δ5G-infected animals, the epitope(s) corresponding to peptides V1V2-9–11 was specific to Δ5G infection (Fig. 5a). As the latter contained the third deglycosylation mutation (Figs 1 and 5b, aa 171), Δ5G specificity was probably secondary to the removal of *N*-glycan at this site in SIV239 gp120 (Fig. 5).

Δ5G-specific Ab responses to linear epitopes in Env elicited immediately following primary infection

In an effort to define the potential relevance of the linear epitope-specific Ab responses in the reduction of acute virus replication in Δ5G-infected animals, we examined the kinetics of Ab reactivity to 12 peptides: Env-10, V1V2-3 and V1V2-9, -10 and -11 for epitopes in region 1; Env-42 and -43 for epitopes in region 2; Env-50 and -51 for epitopes in region 3; Env-56 for epitopes in region 4; and Env-61 and -62 for epitopes in region 5 (Fig. 6). Whilst the induction kinetics of Ab to most peptides were variable in

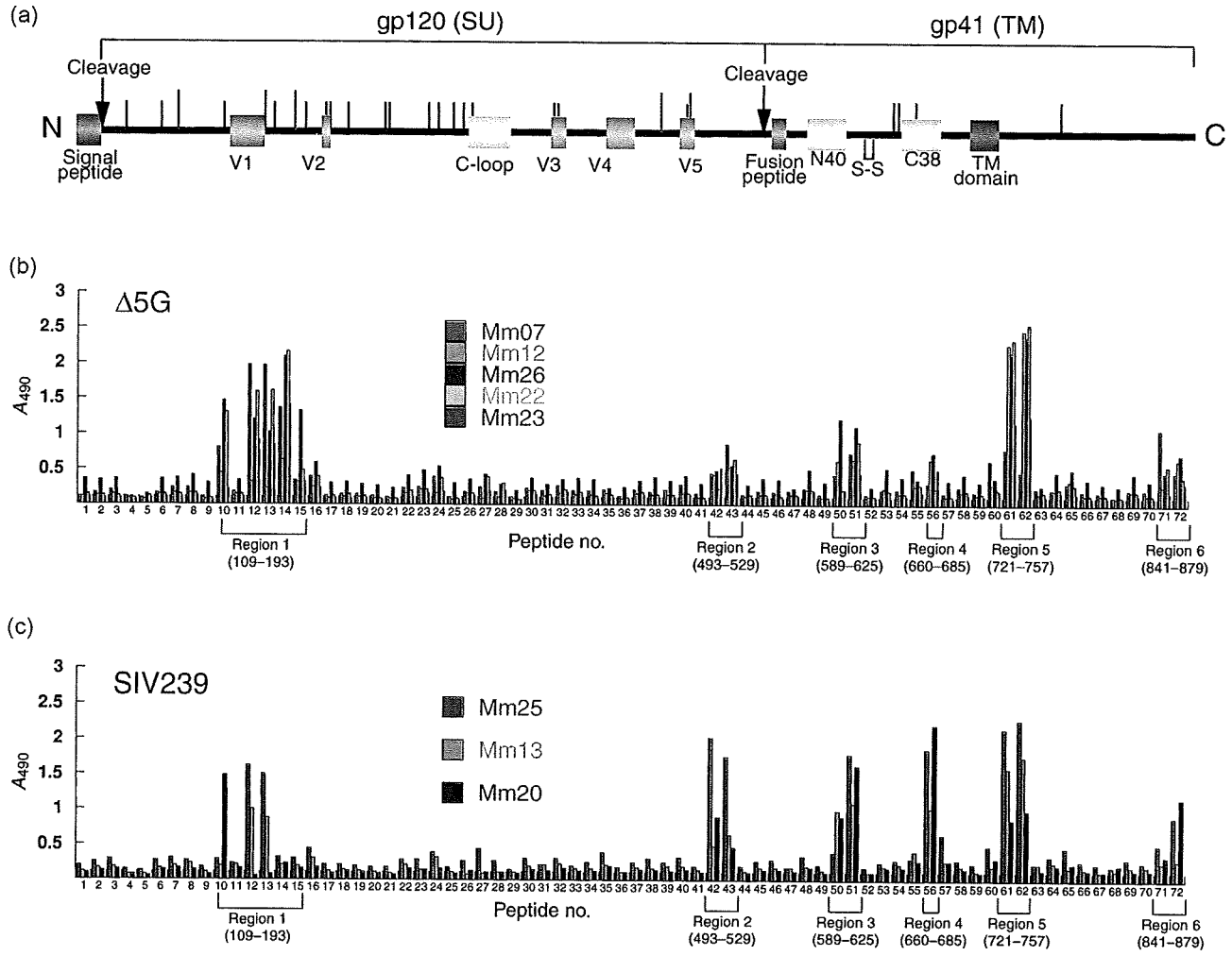

Fig. 4. Ab reactivity to synthetic overlapping peptides spanning the entire Env protein. (a) Diagram of SIV239 Env with the locations of the signal peptide (violet box), variable regions (pink boxes), cysteine loop (yellow box), fusion peptide (green box), N-terminal (N40) and C-terminal (C38) heptad repeats (light-blue boxes), membrane-spanning domain (blue box) and *N*-glycosylation sites (vertical bars) (Burns & Desrosiers, 1991; Choi *et al.*, 1994; Liu *et al.*, 2002). Red vertical bars indicate deglycosylation sites (aa 79, 146, 171, 460 and 479) in Δ5G. S-S indicates the indispensable disulfide bond for hairpin loop formation of the TM protein. (b, c) Plasma samples collected from animals infected with Δ5G (b) and SIV239 (c) at 8 weeks p.i. were used to examine Ab reactivity to 72 peptides (25 mers) overlapping by 13 residues each and spanning the entire Env protein. Reactivity was shown by A_{490}.

plasma from both groups of animals, Ab to V1V2-9, -10 and -11 was specific for Δ5G-infected animals, with rapid induction following primary infection. Ab responses to Env-61 and -62 were also induced rapidly in animals from the two groups; however, it has already been confirmed by SIV and HIV studies that a linear epitope covered by these peptides is the immunodominant epitope with no association with virus control (Eberle *et al.*, 1997; Kent *et al.*, 1992). In contrast to Ab responses to V1/V2 peptides, whilst Ab to peptides Env-51 and -56 in the gp41 ectodomain were detected in SIV239-infected animals, these reactions were low until at least 12 weeks p.i. in Δ5G-infected animals.

Properties of Ab against Δ5G-specific linear epitope

Although Ab reactivity to peptide V1V2-9, -10 and -11 was elicited specifically in Δ5G-infected animals, these Abs were non-nAbs, as these binding Abs were detected in all Δ5G-infected animals, including a nAb-undetectable monkey (Mm26), and before nAb was detected. In addition, we attempted to inhibit neutralization by the addition of excess concentrations of V1V2-9, -10 and -11 to the neutralization assay performed with plasma from Δ5G-infected animals collected at 8 and 12 weeks p.i. The reduction of nAb by the addition of an excess amount of

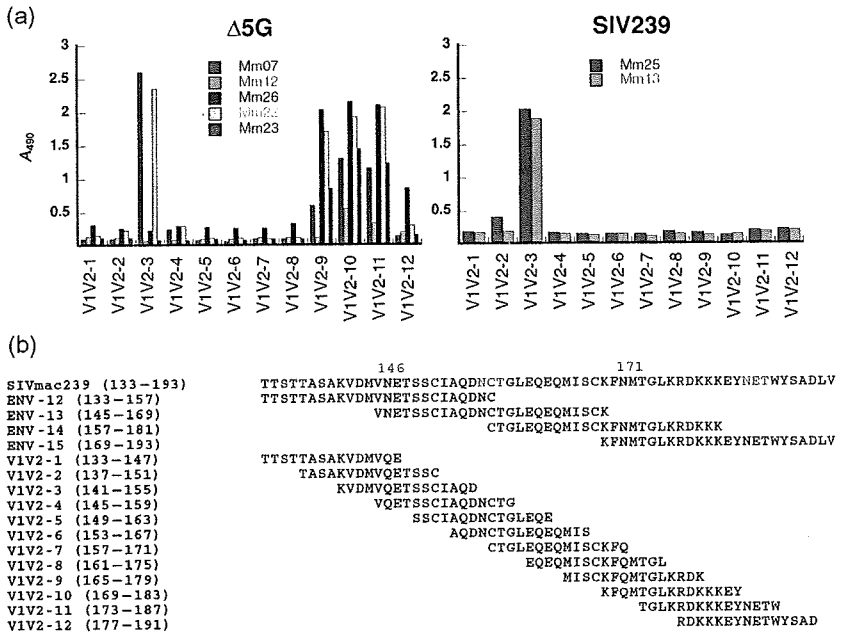

Fig. 5. Ab reactivity to linear epitopes in the V1/V2 region of gp120. (a) To define linear epitopes in the V1/V2 region, peptide ELISA was performed using 12 peptides (15 mers) overlapping by 11 residues each. (b) Sequences and positions of the 12 V1/V2 peptides used in (a) and the peptides Env-12 to -15.

peptide was not detected in any samples, confirming that the epitopes targeted by nAb and V1V2-specific Ab were distinct (data not shown).

Next, we tested plasma IgG samples from SIV-infected animals for the quantitative capture of whole virions. IgG fractions of plasma samples from SIV-infected animals collected at 3–4 weeks p.i. were compared for their capacity to capture Δ5G or SIV239 virions. IgG fractions from two Δ5G-infected animals (Mm07 and Mm22) exhibited remarkably higher virion capture activity than those from other animals (Fig. 7a); however, this capture activity was

Table 1. Epitope-specific Ab-binding regions in Env and influence of deglycosylation on Ab binding

Env subunit	Ab-binding region	Peptide no.	Amino acid range	Region	*P* value*
SU	Region 1	10	109–133	V1	0.6733
		12	133–157	V1	0.5678
		13	145–169	V1/V2	0.5563
		14	157–181	V1/V2	0.0149†
		15	169–193	V1/V2	0.2385
	Region 2	42	493–517	SU C terminus	0.0822
		43	505–529		0.3039
TM	Region 3	50	589–613	Ectodomain	0.4791
		51	601–625		0.0140†
	Region 4	56	660–685	Ectodomain	0.0053‡
	Region 5	61	721–746	Cytoplasmic domain	0.6818
		62	732–757		0.8188
	Region 6	71	841–865	Cytoplasmic domain	0.5237
		72	853–879		0.2451

*A *t*-test was performed by using data in Fig. 4 to determine differences in Ab reactivity between SIV239 infection and Δ5G infection.
†$P<0.05$; ‡$P<0.01$.

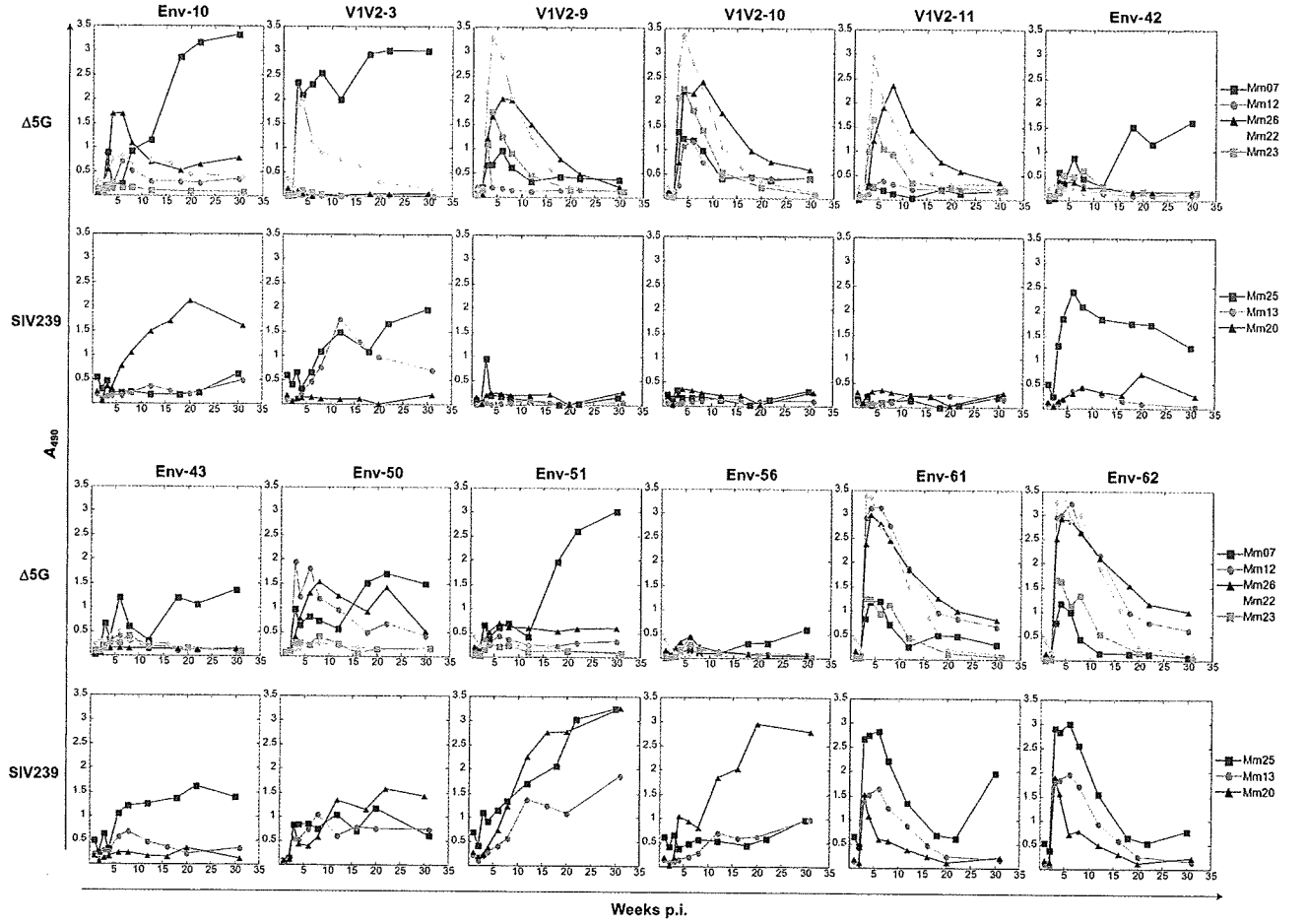

Fig. 6. Kinetics of peptide-specific Ab responses in Δ5G-infected and SIV239-infected animals. The kinetics of Ab reaction against peptides selected in the experiments shown in Figs 4 and 5 was determined as A_{490} using plasma diluted 1 : 100 in an ELISA.

Δ5G-specific, as no appreciable capture of SIV239 virion was detected with these samples. Furthermore, this activity was reduced to the level of control IgG (R374) after selective removal of IgG binding to V1V2-9, -10 and -11 peptides, suggesting that virion capture activity is associated with the Δ5G-specific linear epitope Ab (Fig. 7a). By contrast, IgG fractions from SIV239-infected animals collected at 3–4 weeks p.i. did not exhibit appreciable binding activity either to Δ5G virions or SIV239 virions (Fig. 7b). Thus, these results demonstrated that Δ5G infection elicited not only nAb after 8 weeks p.i., but also a much earlier humoral antiviral mechanism in the form of Δ5G-specific virion-binding Ab at 3–4 weeks p.i. in at least two monkeys (Mm07 and Mm22). To examine the relationship between the two antibody activities, we calculated the correlation of virion capture activity of IgG at 3 or 4 weeks p.i. with a peak nAb titre in Δ5G-infected animals (Fig. 2b) and found that this correlation was statistically significant ($r=1$, $P=0.0167$; Fig. 7c).

DISCUSSION

nAb response in Δ5G-infected animals

Glycosylation of viral spikes has long been recognized as an effective strategy to evade host (humoral) immune surveillance for several pathogens and for HIV/SIV in particular (Dowling *et al.*, 2007; Fournillier *et al.*, 2001; Haigwood & Stamatatos, 2003; Huso *et al.*, 1988; Reitter *et al.*, 1998). In support of these observations, the data presented here demonstrated that quintuple deglycosylation conferred live attenuated vaccine properties to an SIV239 mutant, Δ5G (Mori *et al.*, 2001); however, a cellular but not humoral response was detected as an immune correlate of the protection of Δ5G-infected animals against SIV239 challenge infection. Therefore, we assumed that the complete control of robust acute virus replication in Δ5G-infected animals beyond the initial cell-mediated control would be due to the development of rapid and effective nAbs. This study indicated that, whereas